

**THERMAL-HYDROLOGIC MODELING
PROGRESS REPORT**

Prepared for

**Nuclear Regulatory Commission
Contract NRC-02-97-009**

Prepared by

**Ronald T. Green
Rui Chen
Amit Armstrong
George Rice**

**Center for Nuclear Waste Regulatory Analyses
San Antonio, Texas**

May 1998

CONTENTS

Section	Page
FIGURES	v
TABLES	vii
ACKNOWLEDGMENTS	ix
1 INTRODUCTION	1-1
2 FRAN RIDGE LARGE BLOCK TEST	2-1
2.1 BACKGROUND	2-1
2.2 CENTER FOR NUCLEAR WASTE REGULATORY ANALYSES MODEL DESCRIPTION	2-3
2.3 SIMULATION RESULTS	2-9
3 EXPLORATORY STUDIES FACILITY DRIFT-SCALE HEATER TEST	3-1
3.1 BACKGROUND	3-1
3.2 CENTER FOR NUCLEAR WASTE REGULATORY ANALYSES MODEL DESCRIPTION	3-4
3.3 SIMULATION RESULTS	3-5
4 DRIFT-SCALE REPOSITORY THERMAL-HYDROLOGIC MODELING	4-1
4.1 CENTER FOR NUCLEAR WASTE REGULATORY ANALYSES MODEL DESCRIPTION	4-1
4.2 SIMULATION RESULTS	4-4
5 REFERENCES	5-1

FIGURES

Figure	Page
2-1	Geometry of the large block and locations of the heater boreholes and vertical temperature measurement borehole TT1 (after Wilder et al., 1997) 2-2
2-2	Temperature at TT1-14 (resistance temperature device 14 is within TT1 about 5 cm above the heater plane) as a function of time (after Wilder et al., 1997) 2-3
2-3	Heater power history during rampdown that started on October 6, 1997, and that portion of the subsequent heat up until January 31, 1998. Yellow lines represent measured heater power data. Red circles are data points for this investigation 2-4
2-4	Weekly snapshots of temperature in WT2 (after Wilder et al., 1997) 2-5
2-5	Difference in fraction volume water content in TN3 as a function of depth from top of the block (after Wilder et al., 1997) 2-6
2-6	Geometry and mesh of the MULTIFLO quarter symmetry model, x and y axes are symmetric axes 2-7
2-7	Temperature history at a few points along a vertical line through the center of the three-dimensional large block model 2-10
2-8	Temperature as functions of depth from the top of the block along a vertical line through the center of the three-dimensional large block model 2-10
2-9	Histories of water saturation at a few points along a vertical line through the center of the three-dimensional large block model 2-11
2-10	Water saturation as functions of depth from the top of the block along a vertical line through the center of the three-dimensional large block model 2-11
3-1	Location of the drift-scale test in the exploratory studies facility 3-2
3-2	Schematic of the drift-scale test facility 3-3
3-3	Temperature distribution of the drift-scale test predicted after 4 yr of heating 3-7
3-4	Temperature distribution of the drift-scale test predicted after 5 yr (4 yr of heating and 1 yr of cooling) 3-8
3-5	Extent of the boiling isotherm of the drift-scale test predicted after 4 yr of heating 3-9
3-6	Saturation distribution of the drift-scale test predicted after 4 yr of heating 3-10
3-7	Saturation distribution of the drift-scale test predicted after 5 yr (4 yr of heating and 1 yr of cooling) 3-11
4-1	Temperature profile for a dual continuum simulation of a drift-scale repository model at 0.1 yr 4-5
4-2	Temperature profile for a dual continuum simulation of a drift-scale repository model at 100 yr 4-5
4-3	Temperature profile for a dual continuum simulation of a drift-scale repository model at 1,000 yr 4-6
4-4	Temperature profile for a dual continuum simulation of a drift-scale repository model at 10,000 yr 4-6
4-5	Liquid saturation profile for a dual continuum simulation of a drift-scale repository model at 0.1 yr 4-7
4-6	Liquid saturation profile for a dual continuum simulation of a drift-scale repository model at 100 yr 4-7

FIGURES (cont'd)

Figure		Page
4-7	Liquid saturation profile for a dual continuum simulation of a drift-scale repository model at 1,000 yr	4-8
4-8	Liquid saturation profile for a dual continuum simulation of a drift-scale repository model at 10,000 yr	4-8
4-9	Comparison temperature at the waste package predicted for a dual continuum model and an equivalent continuum model	4-9
4-10	Comparison liquid saturation at the waste package predicted for a dual continuum model and an equivalent continuum model	4-9
4-11	Comparison of dual continuum model and equivalent continuum model predictions, liquid saturation 4 m below the waste package	4-10

TABLES

Table		Page
2-1	Timetable of major events during large block test	2-4
2-2	Matrix thermal and hydrologic properties and fracture hydrologic properties	2-8
3-1	Material and thermal properties for drift-scale heater test simulation [Values taken from Ho and Eaton (1994)]	3-6
4-1a	Matrix properties	4-2
4-1b	Fracture properties	4-3

ACKNOWLEDGMENTS

This report was prepared to document work performed by the Center for Nuclear Waste Regulatory Analyses (CNWRA) for the Nuclear Regulatory Commission (NRC) under Contract No. NRC-02-97-009. The activities reported here were performed on behalf of the NRC Office of Nuclear Material Safety and Safeguards, Division of Waste Management. The report is an independent product of the CNWRA and does not necessarily reflect the views or regulatory position of the NRC.

QUALITY OF DATA, ANALYSES, AND CODE DEVELOPMENT

DATA: No CNWRA-generated original data are contained in this report. Sources for other data should be consulted for determining the level of quality for those data.

ANALYSES AND CODES: MULTIFLO Version 1.2-beta computer code was used for analyses contained in this report. The dual continuum model (DCM) formulation of this computer code is currently undergoing testing and is therefore not under the CNWRA Technical Operation Procedures (TOP)-018.

1 INTRODUCTION

Thermal-hydrologic processes expected to be active at the proposed high-level nuclear waste (HLW) repository at Yucca Mountain (YM) are investigated by simulating three physical systems: (i) the U.S. Department of Energy (DOE) large block test (LBT) at Fran Ridge, (ii) the DOE drift-scale heater test (DST) in the exploratory studies facility (ESF), and (iii) a drift-scale model of the proposed repository. Analyses of the first two systems are designed and conducted to allow comparison of the model results with measurements taken from the field tests. This comparison provides an assessment of the ability of the conceptual and numerical models to simulate thermal-hydrologic processes in geologic media at field scale. If found acceptable, these models can be used to predict thermal-hydrogeologic processes for the proposed repository within a known level of uncertainty. This report summarizes the conceptual and numerical model investigations of the LBT, DST, and drift-scale model of the proposed repository. Subsequent reports will document future developments and interpretations of these modeling investigations.

Analyses for each of the three physical systems are individually introduced and discussed. Included in the introduction for each system is a description of the physical system, conceptual and numerical model definition, boundary and initial conditions, and property assignment. In the cases where the physical system is a field test, observed results from the test are used in the analysis. Available data are currently limited to the LBT. Future analyses will include additional results from the LBT and periodic results from the DST.

All numerical analyses were performed using METRA, the flow component to MULTIFLO. MULTIFLO is a multiphase, multidimensional, nonisothermal heat and mass transfer simulator (Seth and Lichtner, 1996). Different conceptual models are used in this evaluation. Analyses of the LBT and the DST were predicated on an equivalent continuum model (ECM). The conceptual model for the drift-scale model of the repository was based on a DCM, similar to the dual permeability continuum (DKM) formulation used in recent DOE numerical simulations. The DCM formulation is a recent enhancement to MULTIFLO. The drift-scale repository analysis results reported here were also conducted as part of testing the DCM formulation.

2 FRAN RIDGE LARGE BLOCK TEST

2.1 BACKGROUND

The LBT is one of a series of DOE thermal tests that includes laboratory tests of core-size samples, laboratory tests of meter-scale block samples (small block tests), LBT, *in situ* tests [such as the single heater test (SHT) and the DST], and confirmation tests. The LBT is focused on the near-field (NFE) and the altered zone (AZ) environments (Wilder et al., 1997). Objectives of the LBT are (Lin, 1993; Wilder et al., 1997) to assist in understanding the processes that are expected to occur within the NFE and AZ environments, and to provide a test of the models and conceptualizations. The purpose of the LBT is to determine the likelihood of refluxing and the conditions under which it can occur, specifically, to determine if condensate will build up above the boiling zone, dryout will occur, and temperatures will be limited to the boiling point.

The LBT is located on the eastern slope of Fran Ridge, Nevada, Test Site (Wilder, 1997). This site was selected because of its desirable rock type (outcrops of the Topopah Spring tuff), fracture characteristics, and accessibility. The rock at this site is near the interface between the lithophysal and nonlithophysal units of the Topopah Spring tuff and is mineralogically similar to the host rock of the proposed repository.

The size of the LBT is 3 × 3 × 4.5 m. The block was isolated from surrounding rock by an excavation process (Wilder, 1997). Five parallel borehole heaters, each with 450 W power, were installed to approximate a planar heat source. Heater boreholes were drilled with equal spacings of approximately 0.6 m in a horizontal plane (heater plane) at a depth of 2.75 m below the top of the block (figure 2-1). Each heater is 2.44 m long and centered in the heater boreholes. A heat exchanger was installed on the top surface of the block to maintain the temperature at the top boundary at a constant level of 60 °C. An impermeable layer was installed to the sides of the block to minimize moisture flux. Three layers of different insulation materials (Utrottemp, fiberglass building insulation, and Reflectix) were installed on the outside of the moisture barrier to minimize heat loss, and 55 instrument and heater boreholes were sealed either by cement grout, packers, or a Teflon membrane.

An assortment of instruments was installed in the instrument boreholes and on the surface of the block (Lin et al., 1998; Wilder et al., 1997; Blair et al., 1996). The instruments installed in the block include resistance temperature devices (RTDs), rapid evaluation of thermal conductivity and thermal diffusivity (REKA), extensometers and displacement transducers, relative humidity sensors (Humicaps), pressure transducers, neutron logging, and electrical resistivity tomography (ERT) electrodes. Devices mounted on block surfaces include a temperature monitoring system on the top and side surfaces and ERT electrodes on the side surfaces. Heater locations and borehole TT1 are illustrated in figure 2-1.

The measured parameters included temperature, relative humidity, gas pressure, moisture content (using both neutron logging and ERT), thermal conductivity, thermal diffusivity, and displacements (both in boreholes and on fractures on the block surfaces). In addition, coupons of waste package (WP) material and other material were placed in some of the boreholes in the block so that they could be periodically examined; microbes were introduced in the block so that their survivability and migration could be studied; and four observation holes were installed below the heaters to observe water drainage from the heaters through the base of the block.

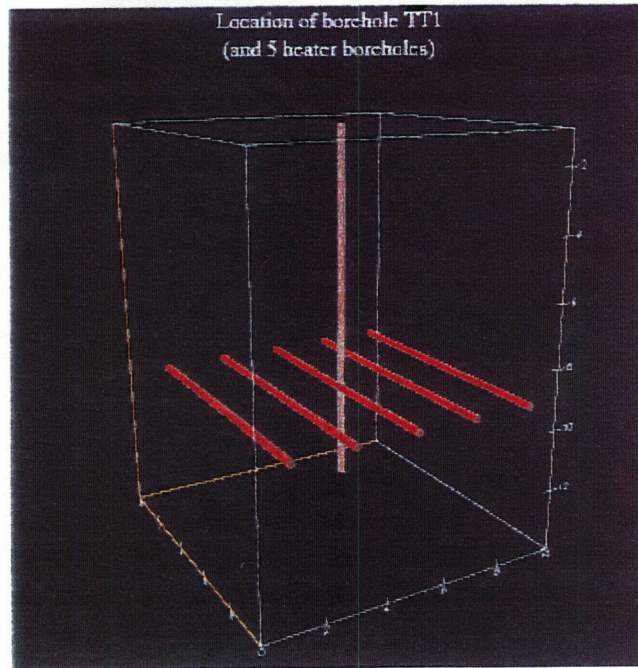


Figure 2-1. Geometry of the large block and locations of the heater boreholes and vertical temperature measurement borehole TT1 (after Wilder et al., 1997)

Each heater was energized to a planned power of 450 W on February 28, 1997 (Lin et al., 1998). Figure 2-2 shows the maximum measured temperature in the block as a function of elapsed time up to October 1, 1997 (Lin et al., 1998), at which time the temperature reached the designed maximum temperature of 140 °C. This was measured by RTD 14 placed in vertical borehole TT1 (1.22 m from the north side and 1.83 m from the east side) at 5 cm above the heater horizon. Most of the depressions in the temperature history curve were due to power outages, however, decreases in temperature at 2,520 and 4,475 hr were possibly associated with rain on June 13 (the June event) and September 2 (the September event), 1997, respectively (Lin et al., 1998).

The heating phase continued until October 6, 1997, followed by a period of heater power rampdown until the end of October and gradual heat up which continued until March 10, 1998 (figure 2-3). The heater power rampdown and subsequent heat up were designed to keep the temperatures in the block at the current levels. A natural cool-down phase began on March 10, 1998, when both the heaters and the heat exchanger were turned off. Table 2-1 lists the major events of the LBT.

Figure 2-4 shows weekly snapshots of the temperature profiles along a horizontal RTD borehole (WT2) drilled from the west side above the heater plane. This figure illustrates that temperature gradually increased after heater power was turned on. It also indicates, along with observations in other horizontal RTD boreholes (Wilder et al., 1997), that the horizontal temperature profiles were fairly flat. This implies that heat losses through the side walls were very small. Refluxing was not observed during the heating phase of the LBT.

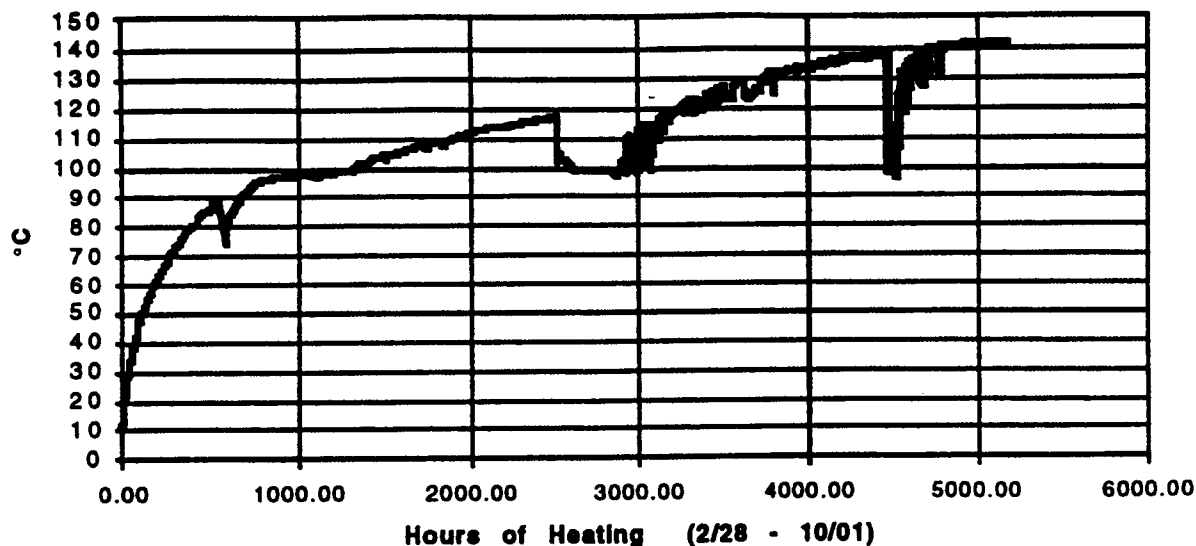


Figure 2-2. Temperature at TT1-14 (resistance temperature device 14 is within TT1 about 5 cm above the heater plane) as a function of time (after Wilder et al., 1997)

Changes in the water content fraction measured with a neutron probe in borehole TN3 are illustrated in figure 2-5 at selected times for the 103-day period after the onset of heating. Borehole TN3 is vertically oriented and located near the center of the block (Lin et al., 1998; Wilder et al., 1997). Since the preheat baseline temperature values have been subtracted, zero fraction water content indicates no change in the moisture content; a positive fraction water indicates an increase in the moisture content; and a negative fraction water content indicates drying. A horizontal line is drawn at the zero fraction volume water to indicate drying and wetting conditions. The development of a drying zone at the heater horizon is depicted by a decrease in the fraction water content. The 0.067 decrease in the fraction water content shown in this figure corresponds to a decrease of 67-percent saturation if the rock porosity is 10 percent. As illustrated, the drying zone began to develop by 48 days of heating. The thickness of the drying zone at this particular borehole location is about 1.0 m. The thickness of the drying zone has been observed to vary with locations (Wilder et al., 1997).

2.2 CENTER FOR NUCLEAR WASTE REGULATORY ANALYSES MODEL DESCRIPTION

A three-dimensional (3D) numerical model was formulated to simulate heat and mass transfer in the LBT. MULTIFLO Version 1.2-beta was used to perform the analyses (Seth and Lichtner, 1996). Using the x-z and y-z planes as planes of symmetry, only a quarter section of the LBT was modeled (figure 2-6). Therefore, only one and one quarter of the five heaters were explicitly modeled. The modeled section corresponds to the northeast quarter of the LBT. To minimize the effect of the uncontrolled boundary at the bottom of the block, the computer model was extended 2 m vertically into the ground. Ideally, simulation should also be extended laterally into the ground, however, this was not an option due to the limitation in geometric modeling in Version 1.2-beta of MULTIFLO. Nevertheless, based on DOE predictive model results, the limitation of not modeling the ground surface beyond the edge of the block should not significantly alter modeling results within the large block.

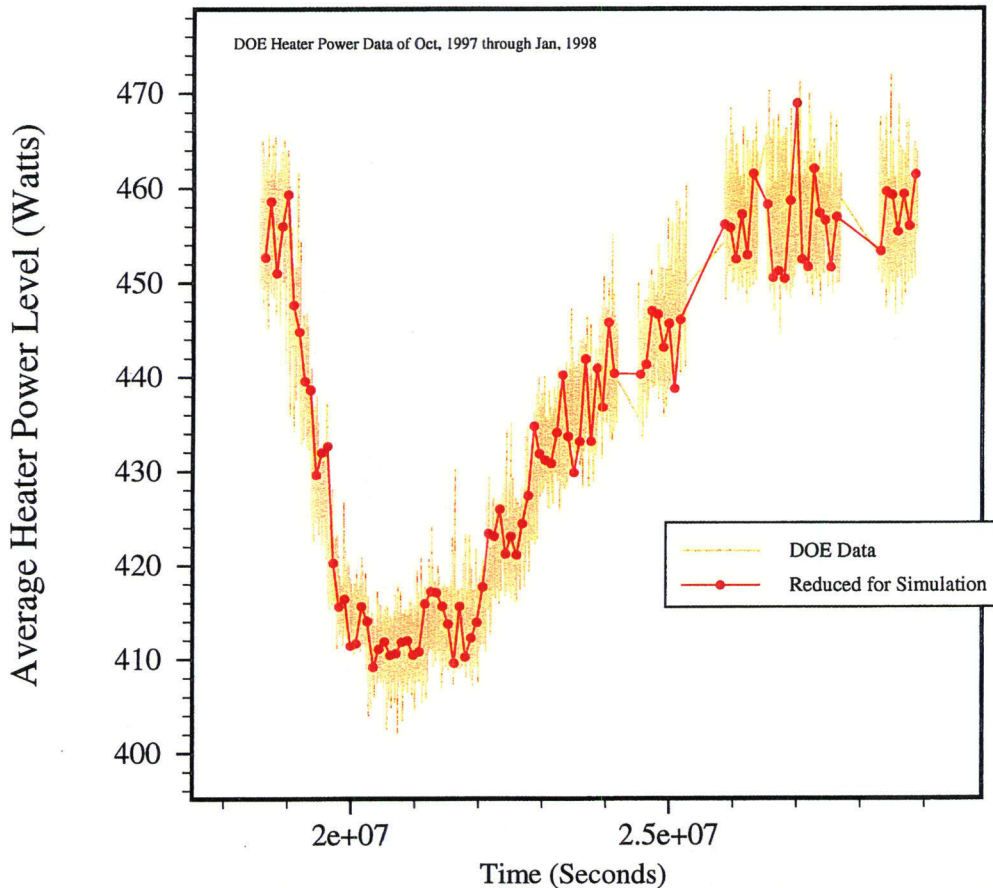


Figure 2-3. Heater power history during rampdown that started on October 6, 1997, and that portion of the subsequent heat up until January 31, 1998. Yellow lines represent measured heater power data. Red circles are data points for this investigation.

Table 2-1. Timetable of major events during large block test

Events	Dates			Remarks
	Absolute Date	Elapsed Hours	Elapsed Days	
Heaters energized	02/28/97 (10 am)	0	0	Heater power is 450 W/heater
June event (first rainfall)	06/13/97	2,520	105	Estimated to be 0.6–0.7 in. at YM, no actual measurement
September event (second rainfall)	09/02/97	4,475	186	Reported 5.0 in. at YM, no actual measurement
Power rampdown	10/06/97 (12 pm)	5,282	220	Power rampdown is followed by a gradual heat up as shown in fig. 2-3.
Natural cooling initiated	03/10/98 (8 a.m.)	8,998	375	Natural cooling is initiated by turning off heater power

9/27

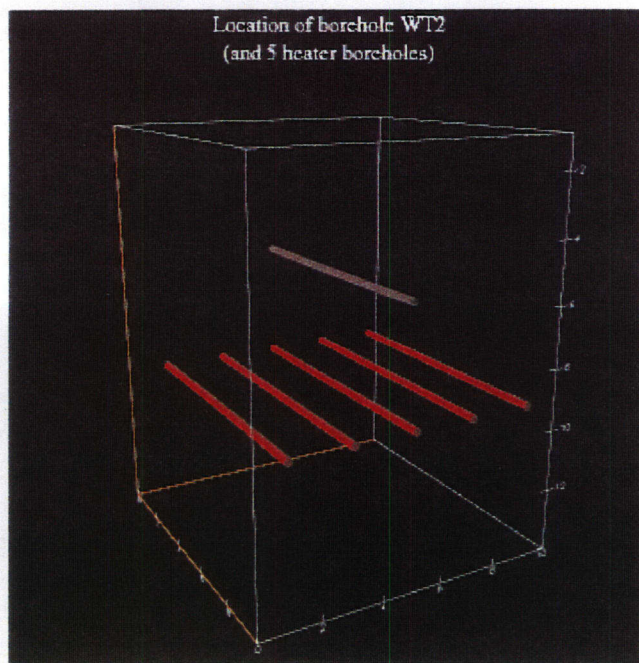
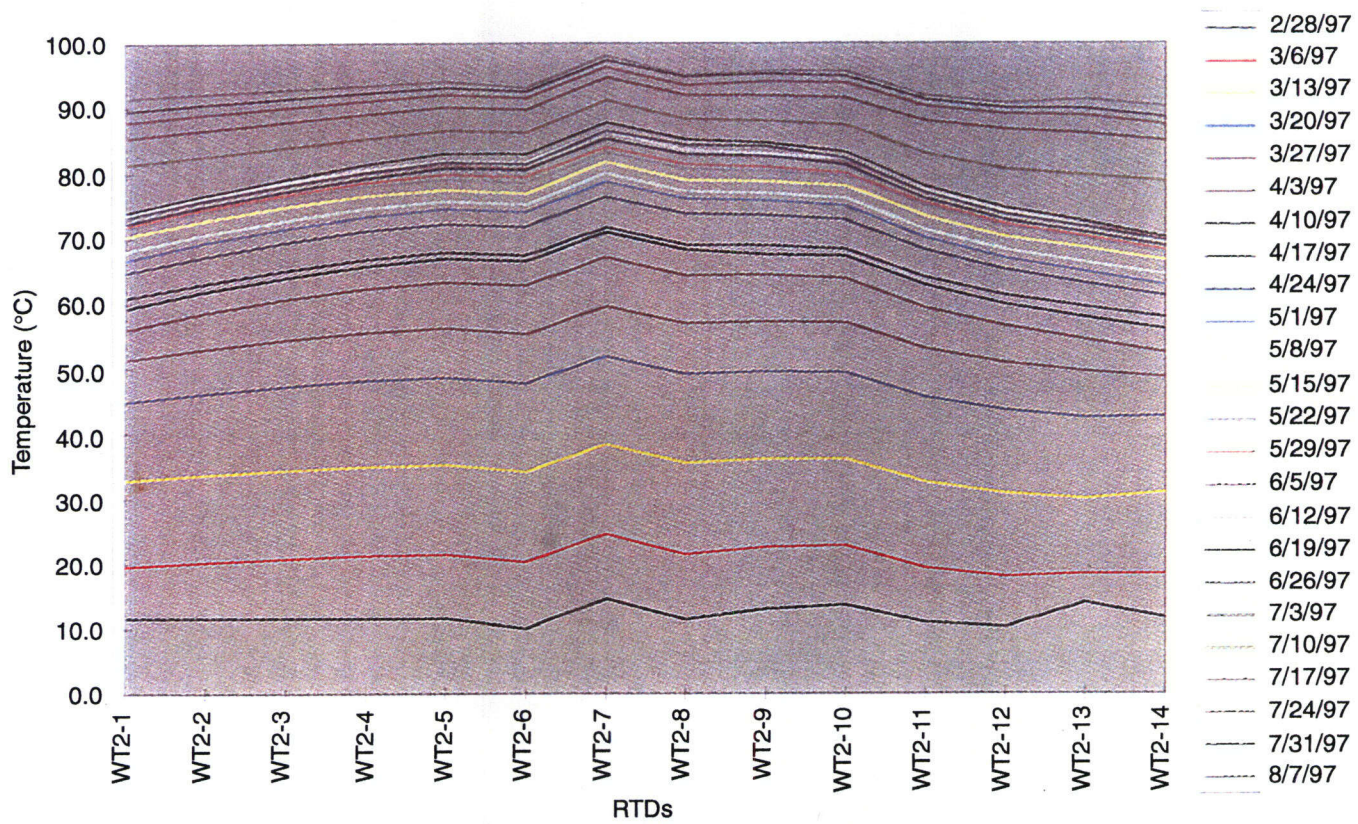


Figure 2-4. Weekly snapshots of temperature in WT2 (after Wilder et al., 1997)

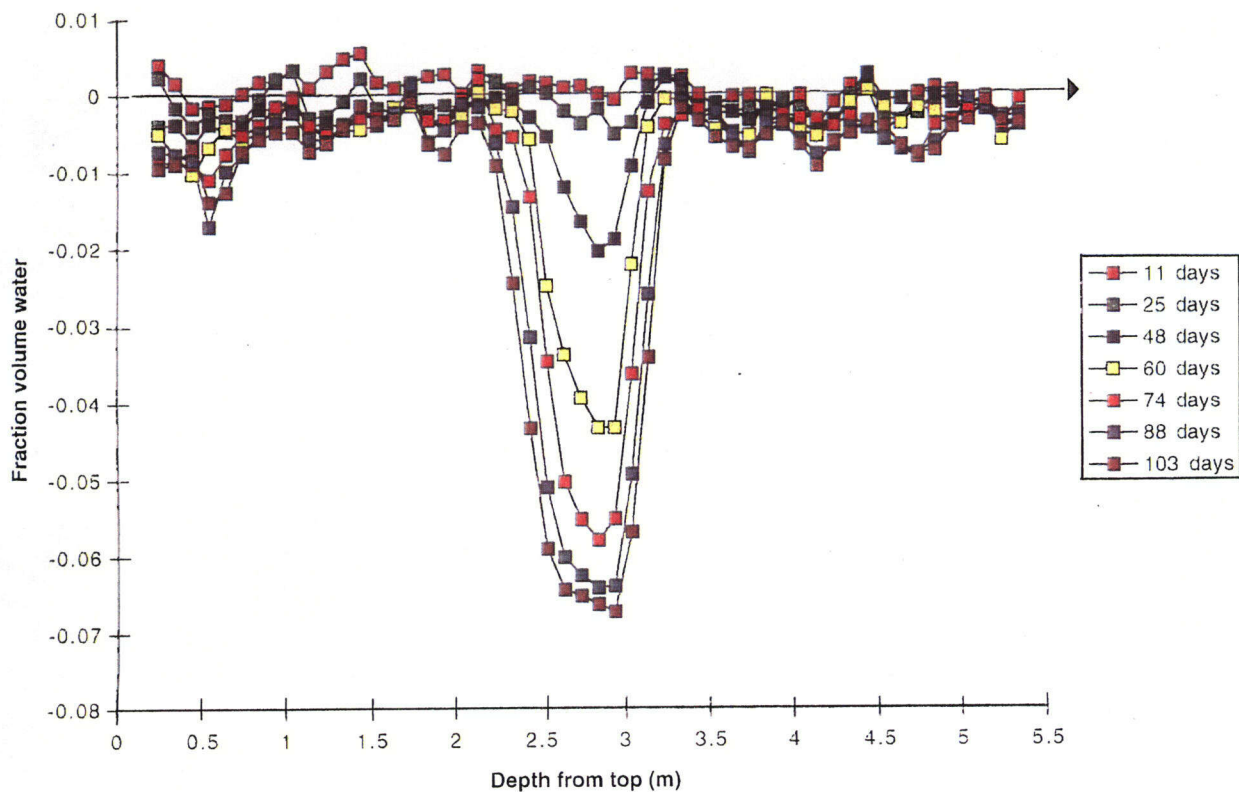


Figure 2-5. Difference in fraction volume water content in TN3 as a function of depth from top of the block (after Wilder et al., 1997)

Temperature at the top boundary was held constant at 60 °C to be consistent with the temperature of the heat exchanger at the top of the block. Limited heat loss through the side wall was incorporated into the model to permit agreement between the model prediction and measured temperature histories at selected locations on the side walls and within the block during the actual field test. Side walls were modeled as no fluid flow boundaries.

The rock block was assumed to be homogeneous and was represented as an ECM. Input property values are presented in table 2-2. Most of these parameters were taken from DOE TSPA-95 (TRW Environmental Safety Systems, Inc., 1995) and pretest predictive analyses (Wilder et al., 1997; Lee, 1995a,b). The bulk permeability was adjusted to approximate the median value obtained by single-borehole air-injection measurements on the block (Wang and Ahlers, 1996; Wilder et al., 1997). None of the input values were modified by calibration.

The initial liquid saturation assumed in this study was 80 percent of pore volume, the approximate median value calculated from single-borehole, air-injection measurements taken during the pretest characterization of the LBT. Property values of the TSw2 were assigned to the model medium (Klavetter and Peters, 1986; Wilder et al., 1997).

10/27

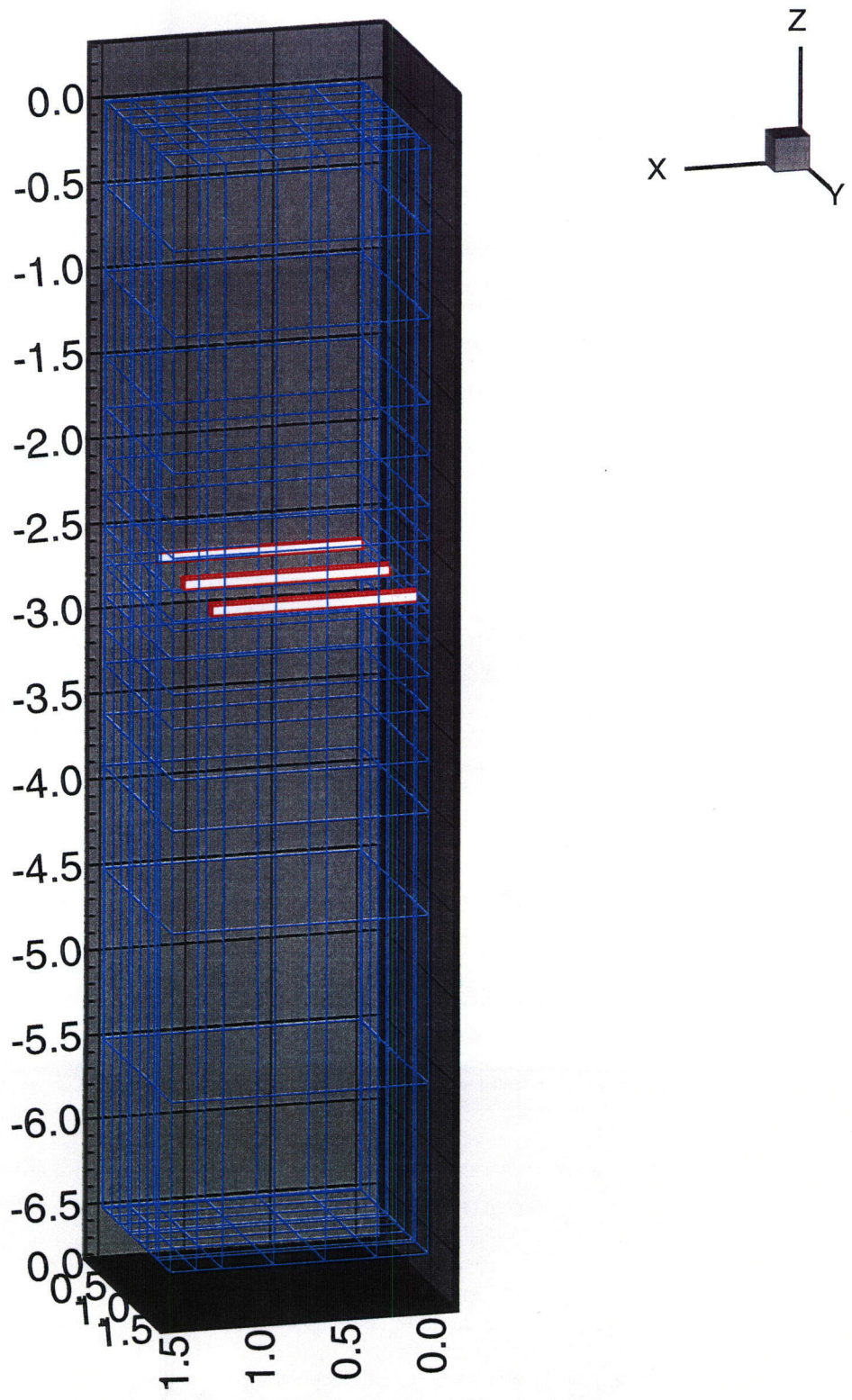


Figure 2-6. Geometry and mesh of the MULTIFLO quarter symmetry model, x and y axes are symmetric axes

The modeling procedure was designed to ensure, to the extent possible, that the simulated heating replicated the heating history of the *in situ* LBT as shown in table 2-1. Rainfall events were not modeled. The block was heated up at 450 W per heater (2,250 W total) for 220 days, followed by a 155-day power rampdown and subsequent heat up (see figure 2-3). It was assumed that power levels in all five borehole heaters were identical and that heat was delivered uniformly along the heated length of each borehole.

Table 2-2. Matrix thermal and hydrologic properties and fracture hydrologic properties

Parameters		Tsw2 ^a	Tsw35 ^b	Tsw ^c
Matrix Thermal and Hydrologic Properties				
Thermal Conductivity (W/m-k)	Dry	2.10	1.56	2.10
	Wet	2.10	2.33	2.78
Specific Heat [J/(kg-K)]		928	948	840
Density (kg/m ³)		–	–	2580
Porosity		0.11	0.11	0.14
Permeability (m ²)		4.00×10^{-18}	1.01×10^{-5}	2.13×10^{-18}
Residual Saturation		–	–	0
van Genuchten Parameters	α (Pa ⁻¹)	6.40×10^{-7}	7.72×10^{-7}	1.36×10^{-6}
	β (–)	1.47	1.47	1.80
Fracture Hydrologic properties				
Porosity (–)		1.19×10^{-9}	2.34×10^{-4}	1.80×10^{-3} ^{c1}
Permeability (m ²)		8.33×10^{-10}	6.55×10^{-9}	3.90×10^{-12} ^{c1}
Residual Saturation (–)		–	–	0.04
van Genuchten Parameters	α (Pa ⁻¹)	1.34×10^{-3}	6.86×10^{-4}	1.31×10^{-3}
	β (–)	3.00	3.00	4.23 ^{c2}
<p>^a Tsw2 properties were obtained from Klavetter and Peters (1986), with some modification by Wilder et al. (1997).</p> <p>^b Tsw34 properties were obtained from Lawrence Berkeley National Laboratory parameter set 4 (Bodvarsson and Bandurraga, 1996) and used by Wilder et al. (1997).</p> <p>^c Tsw properties are presented only for the purpose of comparison. These properties were from TSPA-93 (Andrews et al., 1994) mean with the following exceptions:</p> <p>^{c1} TSPA-93 (Andrews et al., 1994) values lead to excessive computer time. Therefore, these values were taken from TSPA-95 (TRW Environmental Safety Systems, Inc., 1995) table 4.2-2</p> <p>^{c2} Parameter statistics not available in TSPA-93. (Andrews et al., 1994) Values are from TSPA-95 (TRW Environmental Safety Systems, Inc., 1995) table 4.2-2</p>				

2.3 SIMULATION RESULTS

Figure 2-7 illustrates the evolution of temperature at five selected locations along a vertical profile through the center of the block: (i) the center of the heater plane, (ii) 40 cm above the heater plane, (iii) 90 cm above the heater plane, (iv) 50 cm below the top surface, and (v) at the base of the block. The temperature evolution at the heater plane gradually approached the designed maximum temperature of 140 °C. Temperatures at other locations increased to different levels during heating. Temperatures at the base (about 60 °C) and near the top (about 76 °C) of the block attained a steady state after 200 hr of heating and never exceeded the boiling point. Temperatures at and near the heater plane continued to increase until heater power rampdown. Temperature histories for locations 40 and 90 cm above the heater plane and at the heater plane demonstrated a departure from the heating trend when they reached the boiling point. These departures are attributed to a heat-pipe effect, where the zone of vaporization/condensation maintains the temperature at boiling. A second departure from the heating trend was observed at 220 days after the onset of heating. This second feature correlates with the heater power rampdown. Natural cooling is indicated by the constant decrease in temperature after 375 days of heating.

Figure 2-8 illustrates vertical temperature profiles through the center of the block at three specified times: 60, 104, and 375 days after the onset of heating. The 375-day profile correlates with the beginning of the cooling phase. Temperature at the heater plane attained boiling shortly after 60 days of heating. The boiling region never extended beyond about 1 m below or above the heater plane. As illustrated by the flattening of the temperature profile at the boiling point, the effect of the heat pipe is obvious in the last two vertical temperature profiles. However, the effect of a heat pipe is not evident above the heater plane in the temperature profile at the beginning of the cooling phase. The absence of a heat pipe above the heater plane is thought to be attributed to insufficient water saturation to sustain the heat pipe, whereas sufficient water is available below the heater plane.

Figure 2-9 illustrates the evolution of saturation at the same five selected locations for temperature assessment in figure 2-7. Drying is observed at all of the observation location except near the base of the block where condensation appears to have raised the saturation above ambient saturation levels. Figure 2-10 illustrates liquid saturation profiles along a vertical line through the center of the block at 60, 104, and 375 days after the onset of heating. Again, it is noted that all heating was terminated after 375 days of heating. This figure also illustrates drying near the heater plane and various degrees of increased saturation beyond the dryout zone. The width of the dryout zone increased for the duration of heating, from less than 0.5 m at 60 days after heating to about 2 m at the beginning of the cooling phase. Condensation and increased saturation were first observed in the dryout zone below the heater plane after about 60 days of heating and continued until the onset of the cooling phase. Although increased saturation was also observed above the heater plane at 60 days, this elevated level of saturation vanished prior to the onset of cooling.

Simulation results generally compare well with the measurements of the LBT. The temperature evolution near the heater plane (figure 2-7) is similar to the measured temperature history [figure 2-2 for the first 200 days (5,000 hr)]. The effect of a heat pipe is observed in both these figures at about 40–50 days after heating. At about 104 days after the onset of heating, the simulated liquid saturation decreased from the original 80 percent to about 20 percent (figure 2-10). This compares reasonably well with measured data (figure 2-5) that show change in the fraction water content corresponds to about a 67-percent decrease in saturation at about 103 days after heating if the rock porosity is 10 percent.

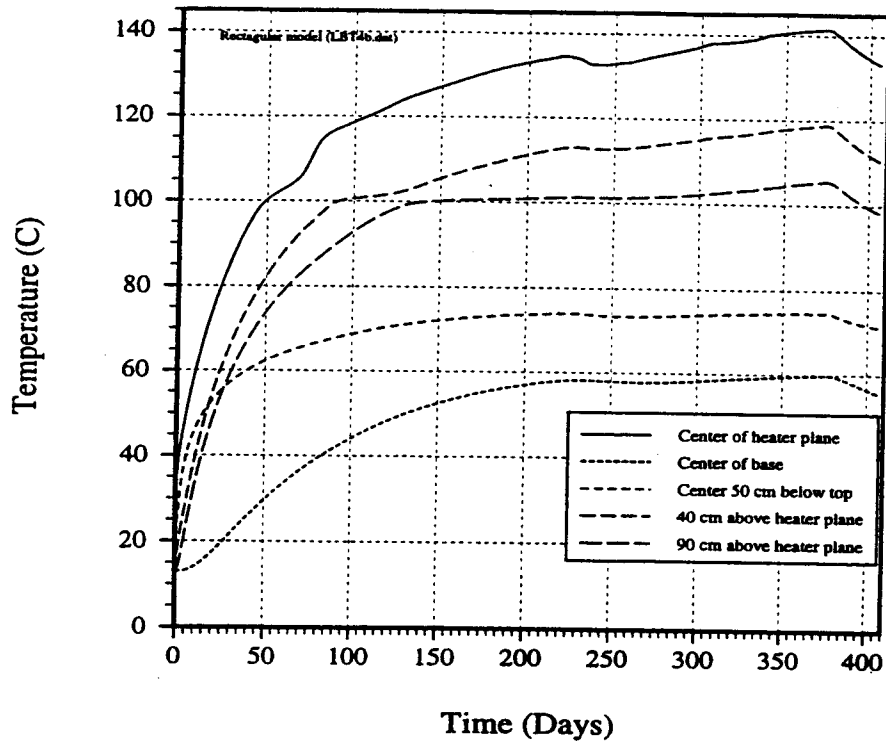


Figure 2-7. Temperature history at a few points along a vertical line through the center of the three-dimensional large block model

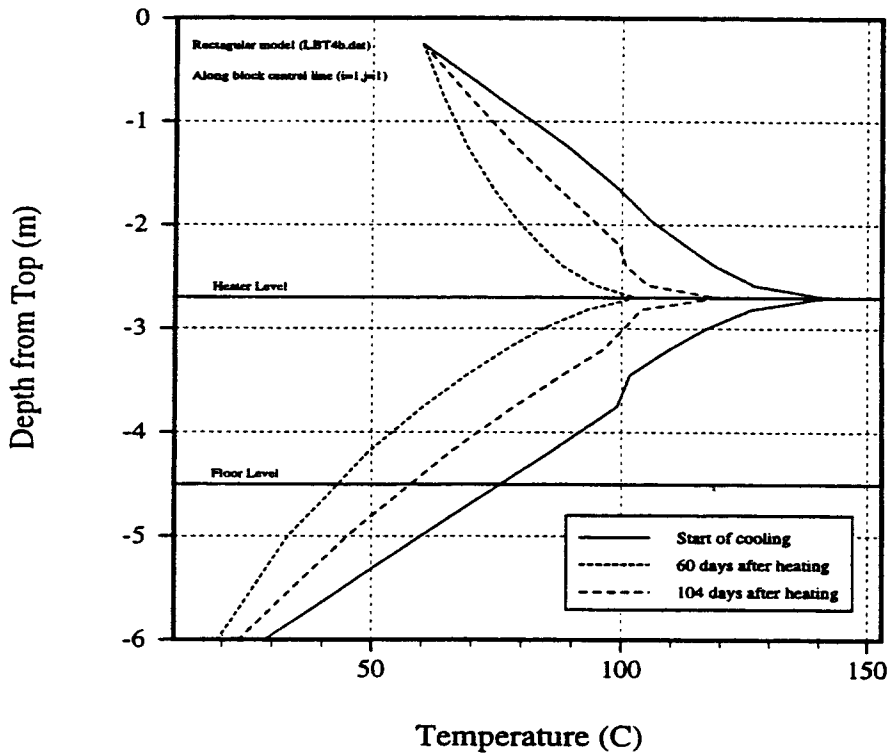


Figure 2-8. Temperature as functions of depth from the top of the block along a vertical line through the center of the three-dimensional large block model

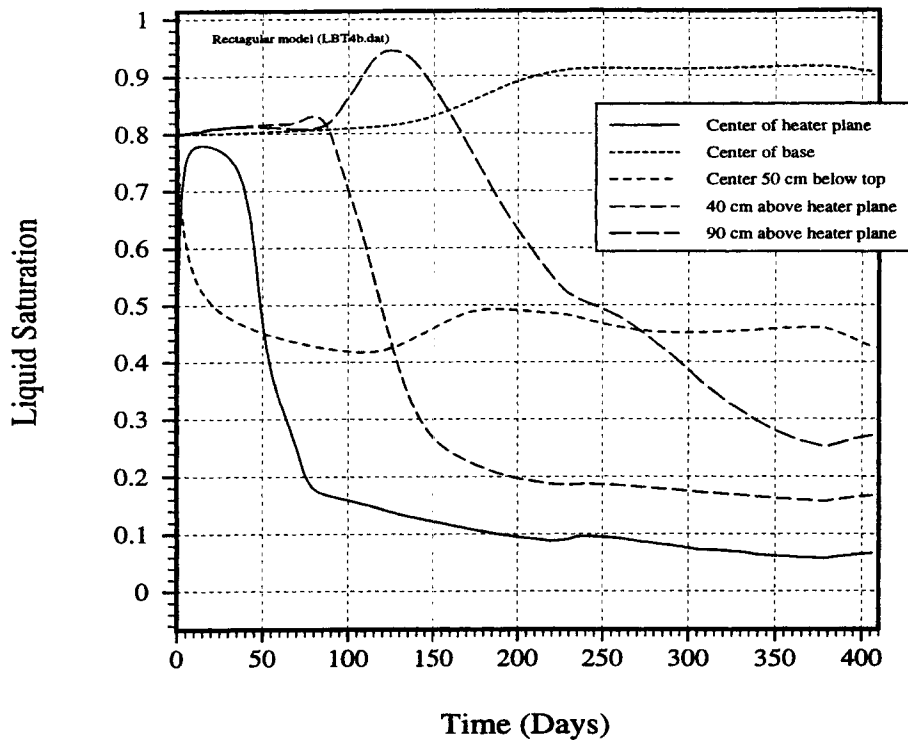


Figure 2-9. Histories of water saturation at a few points along a vertical line through the center of the three-dimensional large block model

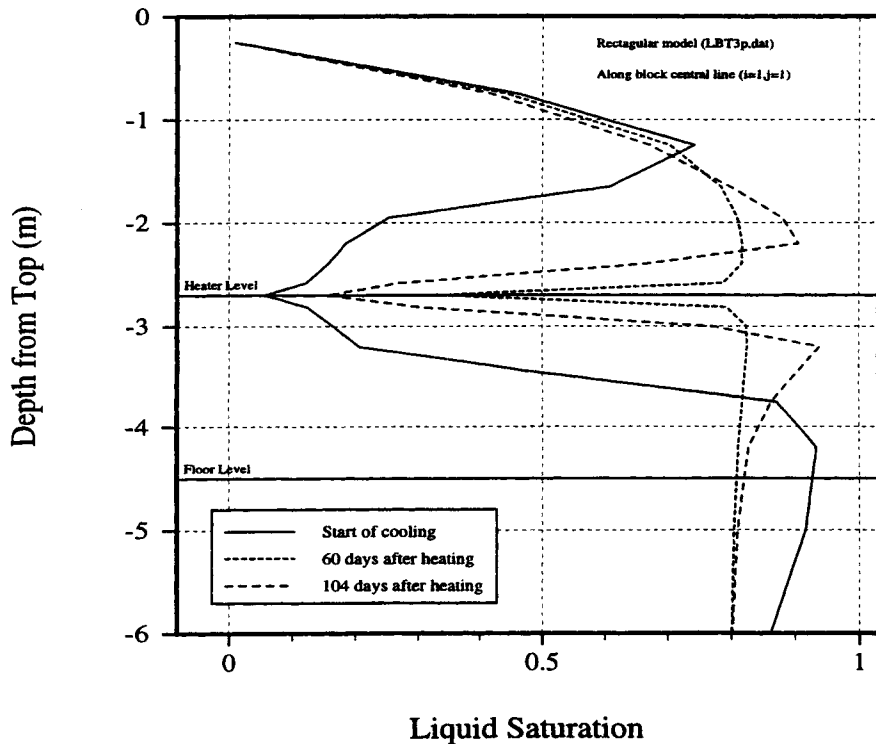


Figure 2-10. Water saturation as functions of depth from the top of the block along a vertical line through the center of the three-dimensional large block model

3 EXPLORATORY STUDIES FACILITY DRIFT-SCALE HEATER TEST

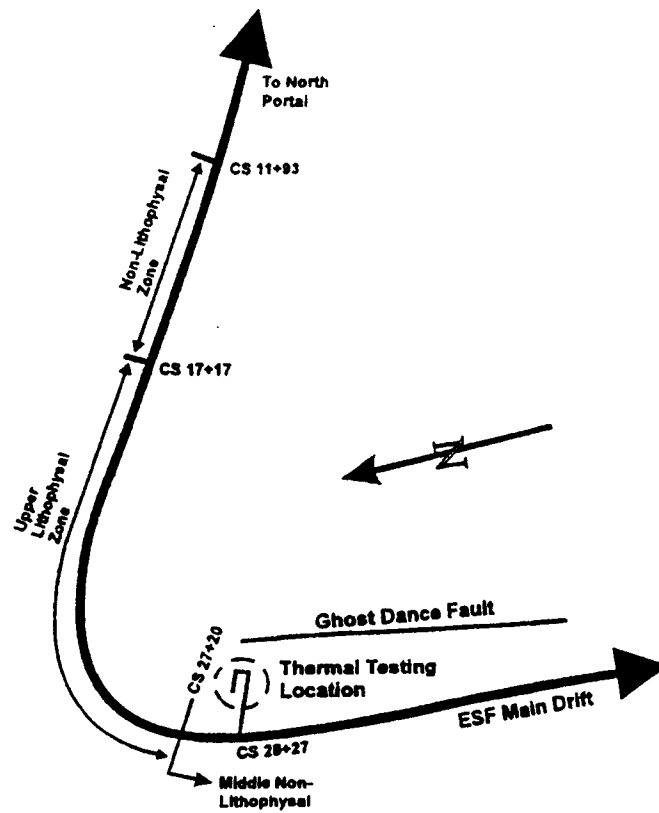
3.1 BACKGROUND

The primary objective of the DST is to develop a better understanding of the *in situ* coupled thermal-mechanical-hydrological-chemical processes in the rock mass surrounding the proposed repository. The test will not be used to replicate the repository environment but will provide an opportunity to observe a rock mass under the influence of repository-like coupled processes. The DST is designed to include a ground support test and emplacement drift thermal test (TRW Environmental Safety Systems, Inc., 1997). This report will only focus on the thermal-hydrological processes expected to be active in the DST. The hydrological objectives of DST can be summarized as (TRW Environmental Safety Systems, Inc., 1997) (i) measure changes in rock saturation (particularly in the drying zone); (ii) monitor the propagation of drying and subsequent re-wetting regions, if any, including potential condensate cap and drainage; (iii) measure change in bulk permeability; and (iv) measure drift-air humidity, temperature, and pressure. The thermal objectives discussed in this report will be limited to temporal and spatial distributions of temperature and saturation and to investigation of the possibility of formation of heat pipes.

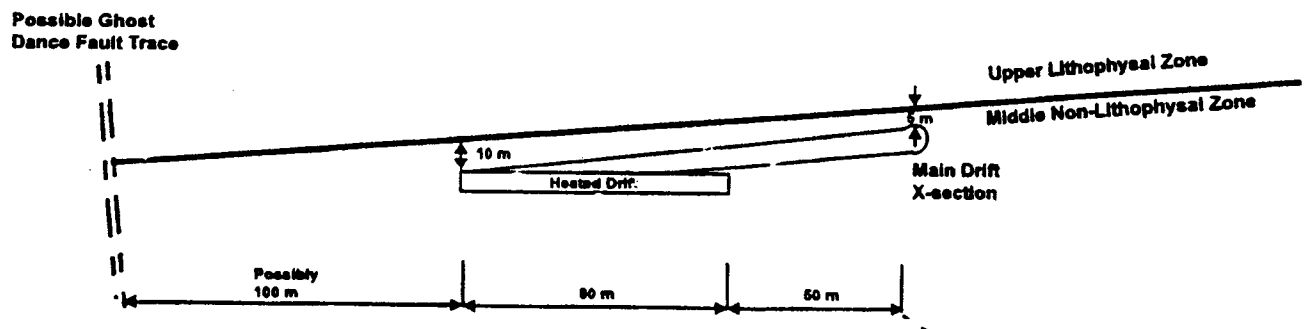
Heating at the DST was initiated on December 8, 1997. The DST is designed to have both a heating and a cooling period. The planned duration of the heating period is 4 yr with a subsequent cooling period also planned for 4 yr. The initial power output is 80 percent of the maximum 54 kW available from the canister heaters (or 43.2 kW) and 100 percent of the maximum 143 kW available from the wing heaters. The maximum nominal temperature along the drift wall will be limited to 200 °C. The heating/cooling schedule will be adjusted to ensure that the DST objectives are satisfied (i.e., that drift-wall temperatures do not exceed 200 °C).

The heater drift is located in the Topopah lithologic unit, which is the primary unit of the proposed repository horizon. The heater test drift is designed and located such that it will not cause an adverse impact to the available area for waste storage and it will not be affected by the interferences from main drift of the ESF. Also, sufficient distance is maintained between the DST and the SHT to prevent inter-test interference. The general location of the DST is presented in figure 3-1, whereas figure 3-2 illustrates a schematic of the thermal test facility. Additional details of the DST design are included in TRW Environmental Safety Systems, Inc. (1997).

The DOE DST analyses are divided into three phases: test scoping, pre-test, and mid/post-test. Test scoping analyses were performed to aid in test design. The pre-test analyses are conducted to provide more comprehensive and realistic simulations of the DST compared to test scoping analyses, particularly when more site-specific data become available. The mid-test analyses will be performed every 6 mo for comparative analysis between the predicted and measured results to refine the various conceptual models and to predict the measurements of the remaining test period. A summation of results provided during pre-test thermal-hydrological analyses by Birkholzer and Tsang (1997), Buscheck et al. (1997), and Francis et al. (1997) and thermo-chemical analyses by Glassley (1997) is included in TRW Environmental Safety Systems, Inc. (1997).



(a) ESF Location



(b) Stratigraphic Location

Figure 3-1. Location of the drift-scale test in the exploratory studies facility

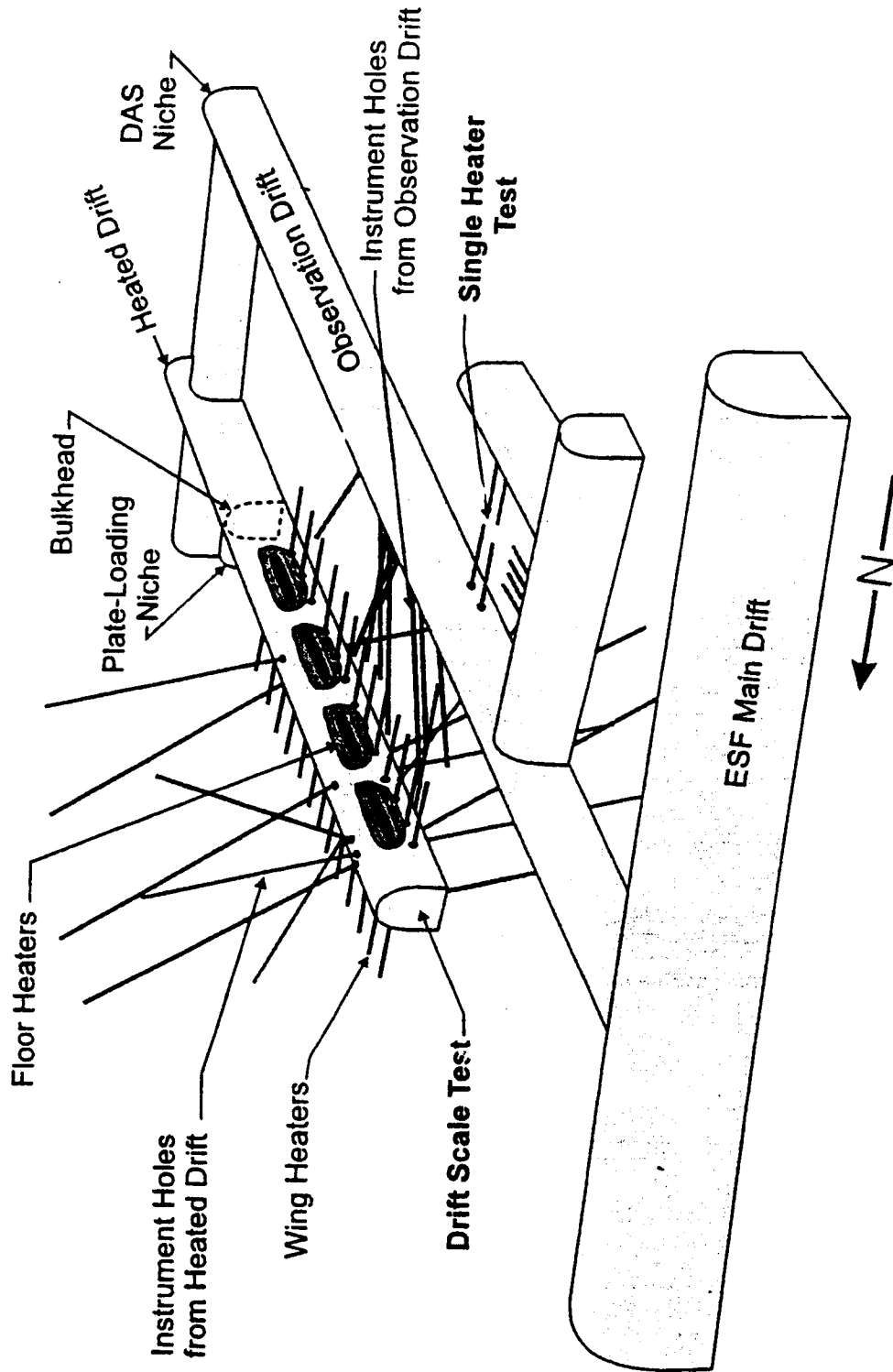


Figure 3-2. Schematic of the drift-scale test facility

Birkholzer and Tsang (1997) performed 3D simulations using a finite difference grid with the TOUGH2 simulator, for both the ECM and DKM formulations, to assess the effects of matrix/fracture interaction and radiative heat exchange. All lateral boundaries of the model domain were modeled as a no-flow boundary for heat, liquid, and gas with the exception of a constant percolation flux introduced at the top boundary. During the simulations, the variations in thermal-hydrologic conditions in the rock mass were analyzed for the impact of different input parameters such as heating rates, percolation flux, and heating schedules. The results indicated that it is desirable, at the beginning, to apply full heating of the test to force a fast response in the DST and then reduce the heating to maintain the temperature at the desired level. It was also concluded that the DST should be a long-term test with at least a 4-yr heating period. This long heating period will provide more complete data on the drying and wetting cycles and will also maintain quasi-steady thermal-hydrologic conditions for a sufficiently long time.

Buscheck et al. (1997) performed 3D simulations for DST using the NUFT simulator. These simulations were performed to study heat-generation rates and heating schedules for the heaters, design of ventilation system, design of thermal bulkhead, design of heaters, and design of instrumentation for monitoring. During these simulations, three percolation flux rates and four different heating schedules were evaluated. Based on modeling results it was concluded that it is important to account for the thermal radiation inside the emplacement drift. Simulations performed with 80 percent of the heating capacity of canister heaters and 100-percent heating capacity of wing heaters indicated that the upper and lower boiling isotherms and dryout zones would be nearly horizontal. However, simulations performed with 80-percent capacity of both canister and wing heaters showed that both the boiling and dryout zones slope toward the lateral edges. The temperatures in the rock mass were found to be very sensitive to the percolation flux. Also, temperatures in the rock mass are influenced by the liquid phase mobility.

Thermal-hydrologic modeling of the DST performed by Francis et al. (1997) used a vertically oriented two-dimensional (2D) (X-Z) cross-sectional model to represent the center of the experiment, a vertically oriented 2D (Y-Z) longitudinal model to characterize edge cooling effects at either end of the drift, and a 3D "periodic boundary" to assess the effects of model dimensionality. Heating was modeled with horizontally placed drift canister heaters and wing heaters with a total power output of approximately 210–220 kW. The drift was heated for 4 yr and allowed to cool for 2 yr in the simulation. The analyses included the prediction of temperatures and displacements at multi-point borehole extensometers (MPBX). Temperature-time history predictions near the center of the experiment, at MPBX-7, -8, -9, and -10, indicated maximum collar temperatures of 260, 300, and 330 °C, respectively, at 2, 3, and 4 yr of heating. Simulations assuming either high- and low-bulk permeability suggested that the constant temperature refluxing zone is driven by buoyant convection. The boiling isotherm (96 °C) contours and liquid saturation profiles indicated a symmetrical dryout zone above and below heater horizon for low permeability simulation, whereas, the high permeability simulation suggested formation of an asymmetric dryout zone with preferential drying below heaters. It was also noted that a large condensate zone formed below the heaters. The 2D models predicted temperatures for the drift wall and surrounding rocks that were consistent with predictions from the 3D periodic model.

3.2 CENTER FOR NUCLEAR WASTE REGULATORY ANALYSES MODEL DESCRIPTION

MULTIFLO Version 1.2-beta with an ECM formulation was used in this report to perform preliminary scoping simulations of the DST. Results will be used to evaluate conceptual models of heat and mass transfer considered for the geologic repository and also to evaluate the various aspects of MULTIFLO. As the DST progresses in time and new data become available, this conceptual model will be refined, or

modified to a DCM formulation, and calibrated so that it can be used for predictive purposes with known levels of uncertainty.

Symmetry of the DST and its heater placement supports the assumption of two vertical planes of symmetry, which allows only one-fourth of the test volume to be modeled. The one-fourth volume domain was discretized into a 3D Cartesian coordinate system with varying block sizes. There are 15 nodes in the x-direction, which runs parallel to the drift longitudinal axis, with lengths of 8, 8, 8, 1, 1, 1, 1, 1, 2, 2, 2, 3, 5, 5, and 25 m. There are 20 nodes in the y-direction, which runs parallel to drifts transverse axis, with lengths of 0.66, 0.66, 0.67, 1, 1, 1, 3, 1, 1, 3, 1, 1, 1, 2, 2, 5, 5, 10, 10, and 50 m. There are 23 nodes in the z-direction, representing elevation, with inter nodal distances of 50, 20, 20, 10, 5, 2, 2, 2, 1, 1, 1, 1, 0.5, 1, 1.5, 1, 1, 1, 2, 10, 20, 20, and 50 m. The applied boundary conditions include no heat or fluid flux across the vertical boundaries. The matrix and fracture continuum is modeled as an ECM. The ECM will provide the combined response of fracture and matrix with the assumption that the properties ascribed to the system represent both.

Both canister floor heaters and wing heaters were represented as a volumetric heat source. Two different heating schemes were used: (i) a total output of 54 kW from the floor heaters and 114.5 kW from the wing heaters and (ii) a total output of the 67.5 kW from the floor heaters and 143.2 kW from the wing heaters. These heating schemes were based on data provided in the TRW Environmental Safety Systems, Inc. (1997) that the total available output of the floor heaters is 68 kW and that of the wing heaters is 143 kW. The air space was modeled as a high porosity medium with high permeability and a low air-entry value. The fracture and matrix property values used in these simulations were taken from Ho and Eaton (1994) and are described in table 3-1. The values are consistent with Wilson et al. (1994) and TRW Environmental Safety Systems, Inc. (1997).

3.3 SIMULATION RESULTS

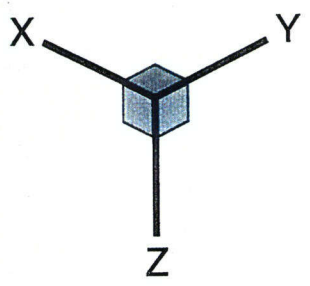
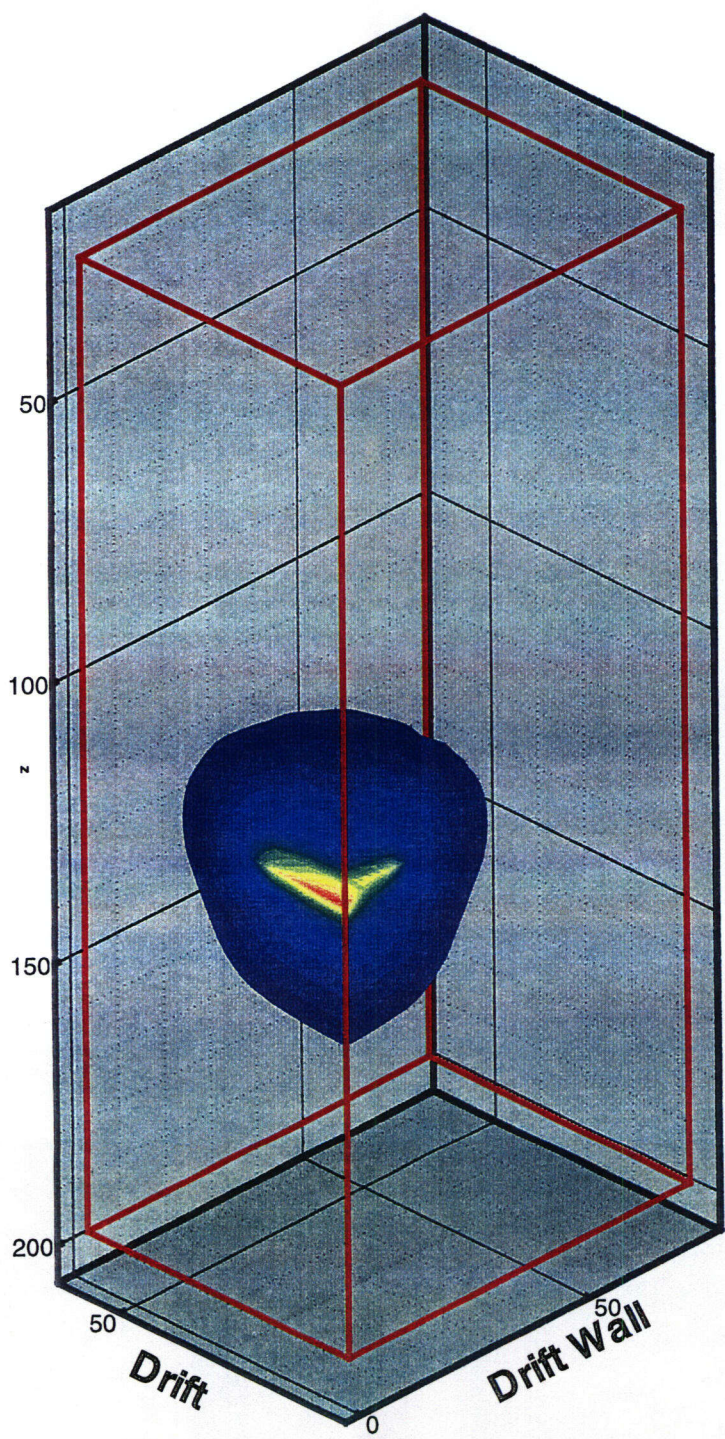
Simulations were performed with the two heating schemes as described in the previous section. Only the results for the heating scheme with higher heat output are discussed in this report. This heating scheme provides higher output than the actual output currently being used for the DST. The temperature distributions at 4 and 5 yr are presented in figures 3-3 and 3-4. The maximum temperature attained after 4 yr was 406.5 °C at the center of the canister heater, however, the maximum temperature after 1 yr of cooling (total time elapsed = 5 yr) was 142.3 °C at the drift wall. The extent of the boiling isotherm (96 °C) after 4 yr of heating is illustrated in figure 3-5. The liquid saturation distribution does not indicate a smooth and symmetrically dryout zone. As shown in figures 3-6 and 3-7, there are some sharp edges which could be indicative of either a coarse discretization or numerical dispersion.

Future analyses will evaluate these preliminary results in greater detail. In these analyses will be an assessment of the refluxing phenomenon, including an evaluation of DST measurements and whether DST instrumentation is effectively monitoring the movement of liquid water near the drift wall. The success of the instrumentation will determine whether refluxing water and seepage into the drift, if present in the DST, can be detected. The ability of the DST instrumentation to detect other processes will be assessed. Of particular interest is whether condensation zones will form either uniformly around the heater drift or preferentially below the drift. There are concerns whether the lack of monitor boreholes and instrumentation in the zone below the drift will prohibit the effective monitoring of the formation of condensation zones. The DCM formulation in MULTIFLO, after the code has been placed under software control, will be used to facilitate the assessment of gravity drainage through fractures. This analysis will assist in predicting the formation of condensate zones around the heater drift.

Table 3-1. Material and thermal properties for drift-scale heater test simulation [Values taken from Ho and Eaton (1994)]

Parameter	Value	Units
Irreducible Liquid Saturation–fracture	0.08	Fraction
Irreducible Liquid Saturation–matrix	0.08	Fraction
λ –fracture	0.4444	–
λ –matrix	0.7619	–
α –fracture	1.3×10^{-4}	Pa^{-1}
α –matrix	5.8×10^{-7}	Pa^{-1}
Porosity–fracture	0.25	Fraction
Porosity–matrix	1.3×10^{-4}	Fraction
Permeability–fracture	1.9×10^{-19}	m^2
Permeability–matrix	2.0×10^{-10}	m^2
Rock Density	2580	kg/m^3
Rock Specific Heat	840.0	$\text{J}/\text{kg}-\text{K}$
Thermal Conductivity (dry)	1.74	$\text{W}/\text{m}-\text{K}$
Thermal Conductivity (wet)	2.3	$\text{W}/\text{m}-\text{K}$
Pore Compressibility	0	Pa^{-1}
Tortuosity	0.5	Fraction

16/27



Temperature (Centigrade)
Distribution After 4 Years

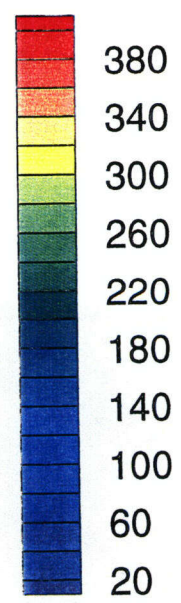
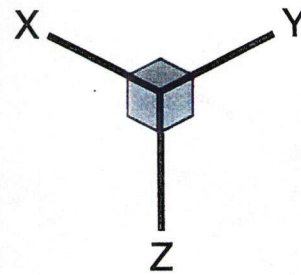
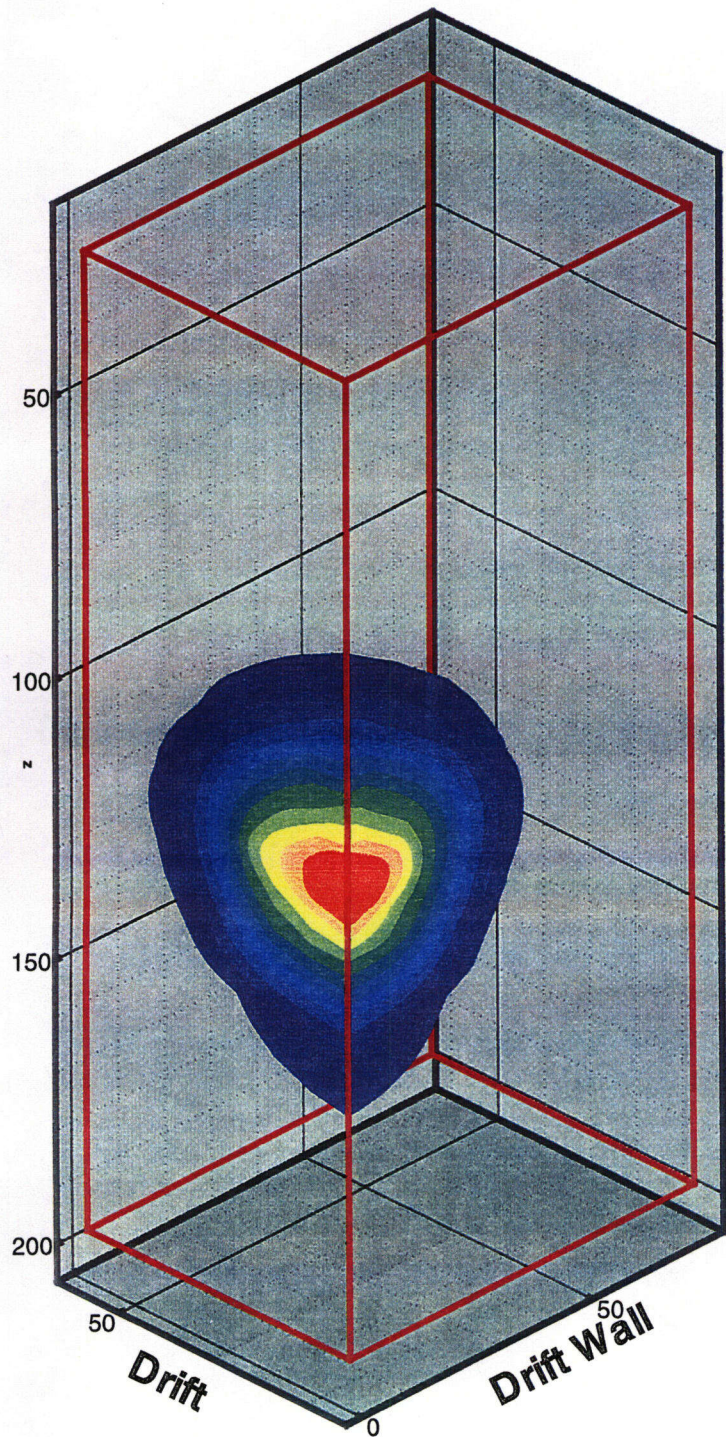


Figure 3-3. Temperature distribution of the drift-scale test predicted after 4 yr of heating



**Temperature (Centigrade)
Distribution After 5 Years**

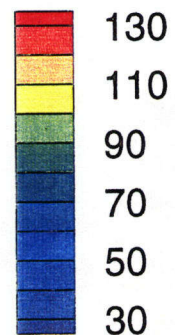


Figure 3-4. Temperature distribution of the drift-scale test predicted after 5 yr (4 yr of heating and 1 yr of cooling)

17/27

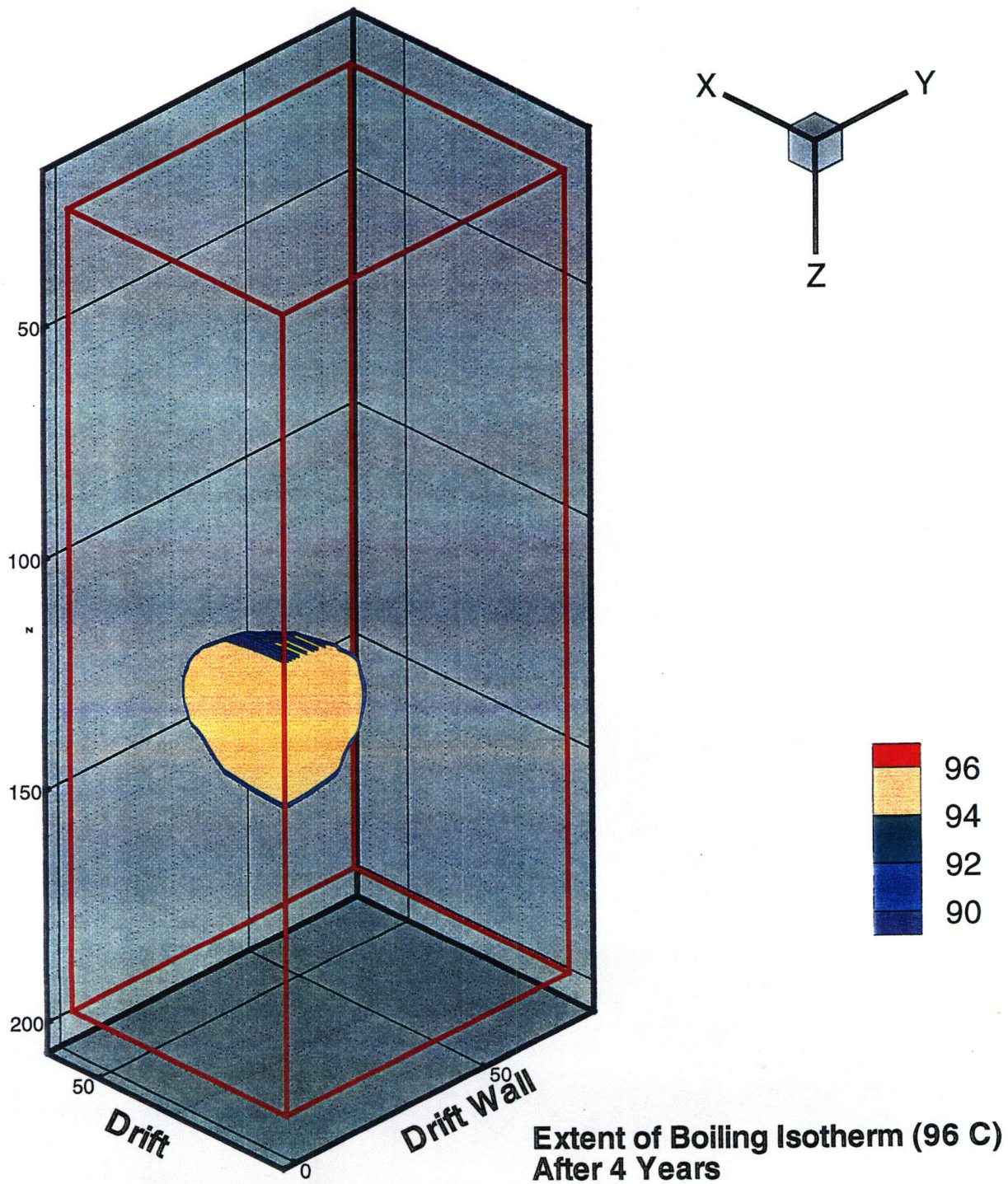
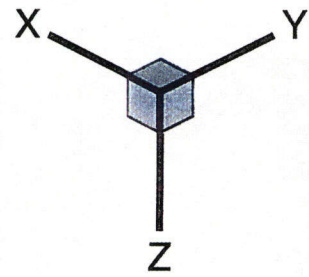
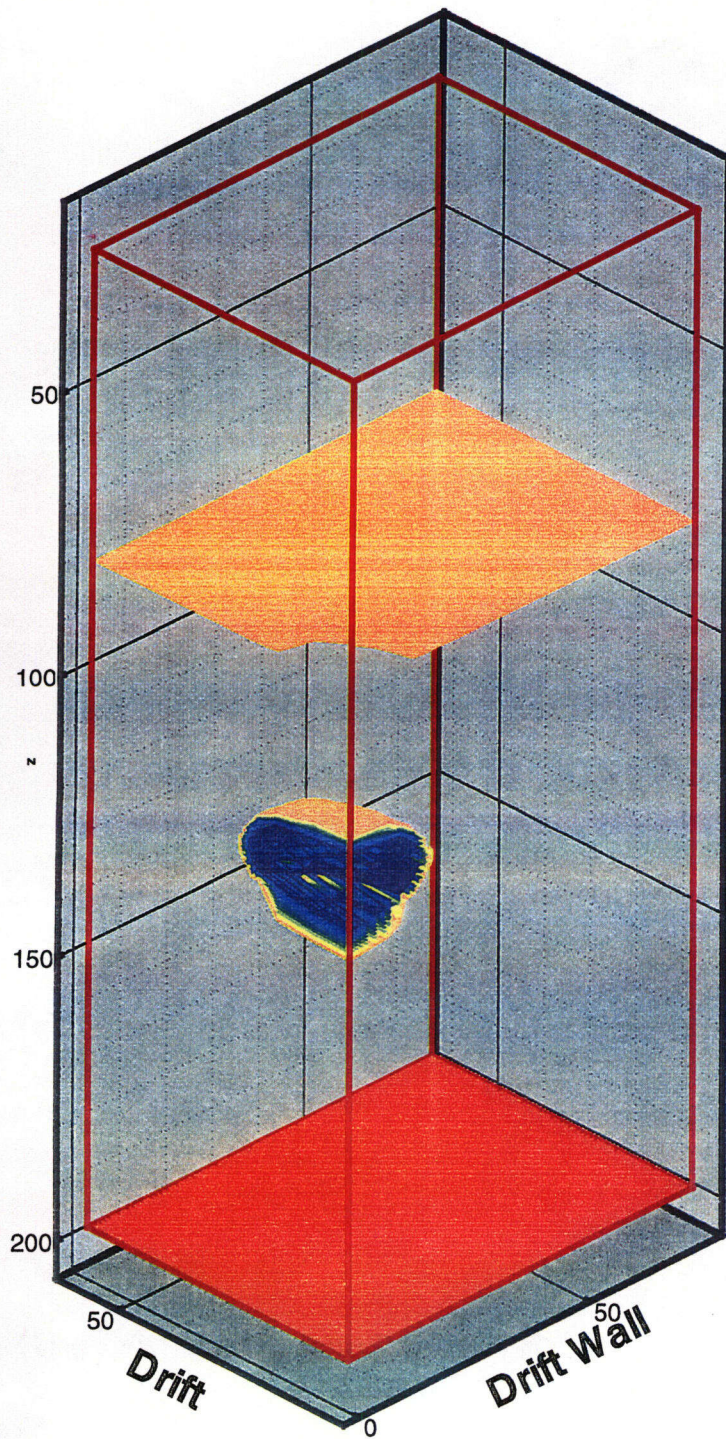


Figure 3-5. Extent of the boiling isotherm of the drift-scale test predicted after 4 yr of heating



**Liquid Saturation
Distribution After 4 Years**

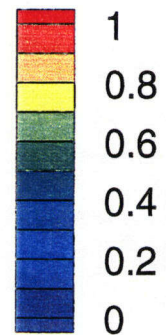


Figure 3-6. Saturation distribution of the drift-scale test predicted after 4 yr of heating

18/27

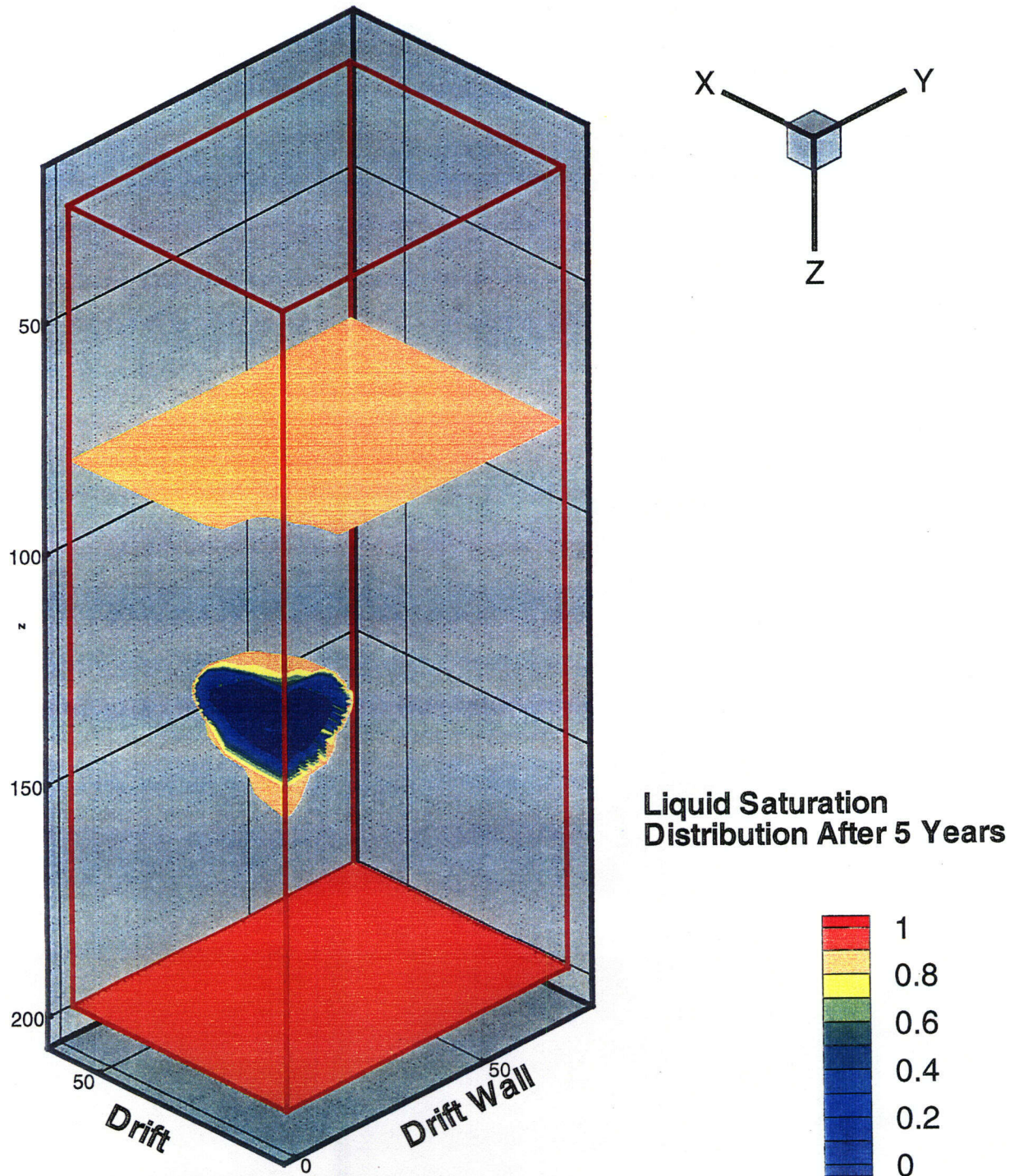


Figure 3-7. Saturation distribution of the drift-scale test predicted after 5 yr (4 yr of heating and 1 yr of cooling)

4 DRIFT-SCALE REPOSITORY THERMAL-HYDROLOGIC MODELING

4.1 CENTER FOR NUCLEAR WASTE REGULATORY ANALYSES MODEL DESCRIPTION

A drift-scale model of the proposed YM repository was formulated to investigate heat and mass transfer mechanisms expected to be active at the proposed repository. The current conceptual model is one-dimensional (1D) and extends from the ground surface into the water table. The heat source was modeled as a horizontally oriented infinite plane centered at the repository horizon. Because of the one dimensionality of the model and the planar heat source, neither the spatial effects of WP and drift spacing nor edge effects were accommodated in this model. The medium was represented as a DCM, one continuum was assigned matrix properties and one continuum was assigned fracture properties. Heat transfer between the two continua is instantaneous, however, mass transfer is delayed by a transfer term. It is the introduction of the transfer term that permits the assumption of hydraulic equilibrium in the ECM to be avoided.

The modeled column is representative of the area located to the west of the Ghost Dance Fault. The stratigraphic section is described in Bodvarsson and Bandurraga (1996). The section consists of 21 stratigraphic units with a total thickness of 517 m from the Tiva Canyon to the Prow Pass. Permeabilities and van Genuchten parameters for the 42 material types (21 matrix and 21 fracture) were taken from measured values reported in Bodvarsson et al. (1997). Values for porosities, residual saturations, and thermal properties were taken from measured values reported in the two most recent DOE performance assessments (Wilson et al., 1994; TRW Environmental Safety Systems, Inc., 1995). The 1D numerical model has a total of 62 elements that range in thickness from 1.6 m thick at the repository horizon to a maximum of 10.0 m thick at ground surface and 5.0 m thick at the model base. Both fracture and matrix elements have the same dimensions. A summary of the 21 stratigraphic units, thicknesses, and matrix and fracture properties is included in tables 4-1a and 4-1b, respectively.

An average infiltration of 1 mm/yr was applied to the upper boundary. The DCM formulation for MULTIFLO currently applies all surface infiltration to the matrix. The relative properties of the matrix and fracture components to the surface boundary element determine whether the infiltrating water enters the fracture system or remains in the matrix. The 1D DCM model was run to steady state (i.e., 100,000 yr) with an infiltration of 1 mm/yr and an imposed geothermal gradient of 0.027 K/m, from 13 °C at the surface to 27 °C at the water table, prior to the onset of heating.

A heat source of 83 kW/acre was specified at a depth of 183 m from the surface. The heat source was assumed as uniform across the entire repository. The initial heat load of 83 kW/acre decays after the onset of heating. The rate of decay was approximately exponential and was taken from TRW Environmental Safety Systems, Inc. (1995). The effects of the drift-air space, ground support, and backfill material were not included in the 1D model.

Drift-scale repository simulations were also performed using a 1D ECM formulation for comparison with results of the DCM simulations. The two conceptual models were assigned the same unit dimensions, material properties, and boundary conditions. The ECM model was also run to steady state (100,000 yr) prior to the onset of heating at an initial heat load of 83 kW/acre at the repository.

Table 4-1a. Matrix properties

Unit	Thickness (m)	Porosity (-)	Permeability (m ²)	α (Pa ⁻¹)	n (-)	Thermal Conductivity (W/m-K)
TCw11	40	0.087	5.4×10^{-18}	1.17×10^{-6}	0.232	1.69
TCw12	6	0.087	5.4×10^{-18}	1.32×10^{-6}	0.236	1.69
TCw13	3	0.087	4.9×10^{-17}	6.46×10^{-7}	0.427	1.69
PTn21	3	0.421	3.1×10^{-14}	3.80×10^{-5}	0.231	0.61
PTn23	3	0.421	8.3×10^{-14}	4.57×10^{-5}	0.287	0.61
PTn24	5.5	0.421	1.1×10^{-13}	4.27×10^{-5}	0.349	0.61
PTn25	13	0.421	2.5×10^{-13}	1.95×10^{-4}	0.279	0.61
TSw31	3.5	0.139	4.9×10^{-17}	1.00×10^{-5}	0.237	2.10
TSw32	40	0.139	2.8×10^{-16}	2.29×10^{-5}	0.273	2.10
TSW33	25.5	0.139	1.1×10^{-17}	6.67×10^{-6}	0.247	2.10
TSw34	8	0.139	4.1×10^{-18}	1.02×10^{-6}	0.322	2.10
TSw35	65.5	0.139	1.5×10^{-17}	3.31×10^{-6}	0.229	2.10
TSw36	98	0.139	8.9×10^{-17}	7.41×10^{-7}	0.414	2.10
TSw37	24	0.139	1.3×10^{-17}	1.55×10^{-6}	0.387	2.10
CH1vc	27.5	0.331	1.3×10^{-12}	6.61×10^{-5}	0.190	1.28
CH1zc	27.5	0.306	1.4×10^{-17}	8.32×10^{-7}	0.366	1.42
CH2zc	16	0.306	9.1×10^{-18}	1.95×10^{-6}	0.220	1.42
CH3zc	47	0.306	9.1×10^{-18}	1.95×10^{-6}	0.220	1.42
CH4zc	18.5	0.306	1.5×10^{-17}	7.76×10^{-6}	0.477	1.42
PP3vp	37.5	0.306	2.8×10^{-15}	1.74×10^{-5}	0.311	2.10
PP2zp	5	0.306	5.8×10^{-17}	1.66×10^{-6}	0.316	2.10

Table 4-1b. Fracture properties

Unit	Thickness (m)	Porosity (-)	Permeability (m ²)	α (Pa ⁻¹)	n (-)	Thermal Conductivity (W/m-K)
TCw11	40	0.018	6.0×10^{-12}	2.95×10^{-4}	0.492	1.69
TCw12	6	0.018	6.0×10^{-12}	2.95×10^{-4}	0.492	1.69
TCw13	3	0.018	2.4×10^{-12}	9.12×10^{-5}	0.492	1.69
PTn21	3	0.018	3.0×10^{-13}	1.10×10^{-3}	0.492	0.61
PTn23	3	0.018	2.9×10^{-12}	3.39×10^{-3}	0.492	0.61
PTn24	5.5	0.018	1.2×10^{-13}	9.33×10^{-4}	0.492	0.61
PTn25	13	0.018	2.5×10^{-13}	1.95×10^{-4}	0.279	0.61
TSw31	3.5	0.018	1.7×10^{-12}	3.98×10^{-5}	0.481	2.10
TSw32	40	0.018	1.8×10^{-12}	9.33×10^{-5}	0.488	2.10
TSW33	25.5	0.018	8.9×10^{-13}	1.78×10^{-4}	0.492	2.10
TSw34	8	0.018	4.5×10^{-13}	9.77×10^{-5}	0.492	2.10
TSw35	65.5	0.018	1.4×10^{-12}	1.10×10^{-4}	0.492	2.10
TSw36	98	0.018	1.2×10^{-12}	1.32×10^{-4}	0.492	2.10
TSw37	24	0.018	1.2×10^{-12}	1.17×10^{-4}	0.492	2.10
CH1vc	27.5	0.018	1.7×10^{-13}	1.17×10^{-3}	0.492	1.28
CH1zc	27.5	0.018	2.4×10^{-14}	1.12×10^{-3}	0.492	1.42
CH2zc	16	0.018	1.2×10^{-14}	1.23×10^{-3}	0.492	1.42
CH3zc	47	0.018	1.2×10^{-14}	1.23×10^{-3}	0.492	1.42
CH4zc	18.5	0.018	1.5×10^{-14}	1.15×10^{-3}	0.492	1.42
PP3vp	37.5	0.018	6.9×10^{-13}	1.41×10^{-3}	0.492	2.10
PP2zp	5	0.018	6.5×10^{-14}	3.72×10^{-4}	0.492	2.10

4.2 SIMULATION RESULTS

Preliminary predictions of temperature and saturation for the drift-scale repository DCM simulations at 0.1, 100, 1,000, and 10,000 yr are illustrated in figures 4-1 through 4-8, respectively. Figures 4-1 through 4-4 display temperature as a function of depth. The temperature at the WP (depth = 183 m) reached 100 °C by 12 yr, and remained above 100 °C for approximately 1,700 yr after the onset of heating. A maximum WP temperature of 127 °C was reached at 220 yr. The thickness of the zone where temperatures exceeded 100 °C increased from about 80 m at 100 yr to about 200 m at 1,000 yr, then disappeared by 1,700 yr. Temperatures in adjacent fracture and matrix elements were always the same.

Fracture and matrix saturations are illustrated in figures 4-5 through 4-8 for the four times. At all depths and times, fracture saturations were less than or equal to matrix saturations. Fracture and matrix saturations were only equal at locations where the rock was either completely dry or completely saturated.

Saturations in both the fractures and the matrix remained relatively constant in the upper 100 m of the profile subsequent to the onset of heating. As expected, saturations varied considerably around the repository horizon. Near the repository, the zone where matrix saturation was less than 50 percent grew from less than 10 m thick at 0.1 yr, to about 50 m thick at 1,000 yr. At 10,000 yr, the thickness of this relatively dry zone was again less than 10 m. Fracture saturations above and below the repository horizon fluctuated over a range from 0 to about 40 percent before returning to their pre-heat saturation values by 10,000 yr.

Increases in fracture saturation appear to be associated with corresponding increases in matrix saturation. At 100 yr, the increased fracture saturations at a depth of 150 to 180 m, and from 220 to 320 m corresponded with saturated conditions in the matrix at the same depth. At 1,000 yr, the increased fracture saturations between about 400 and 450 m also corresponded with the depths at which the matrix was saturated. Fracture saturations at 10,000 yr were about the same as they were at the onset of heating. On the other hand, overall saturation levels in the matrix decreased by 10,000 yr relative to the pre-heat matrix saturations.

Results of the DCM simulation were compared with the results of a comparable ECM simulation. Temperatures predicted by the two methods are different (figure 4-9). The peak temperature predicted by the DCM method is 127 °C at 220 yr, while the peak predicted by the ECM method is 151 °C at 900 yr. The DCM method predicted the temperature at the WP would remain above 100 °C for about 1,700 yr, while the ECM predicted about 6,200 yr.

Matrix saturations predicted by the DCM and ECM methods are similar. In general, the fluctuations predicted along the profile by the DCM are also predicted by the ECM. Figure 4-10 shows temporal variations in saturation at the WP. Both methods predicted that the WP will be nearly unsaturated for most of the simulation. However, at early and late times, matrix saturations predicted by the DCM method were higher than those predicted by the ECM method. Figure 4-11 shows matrix saturations immediately (4 m) below the WP. Saturations predicted by the DCM method were initially about 15 percent higher than those predicted by the ECM method. Between about 50 and 1,000 yr, predicted saturations were nearly equal. After 1,000 yr, saturations predicted by the DCM method increased relative to those predicted by the ECM method. At 10,000 yr, DCM saturations were about 30 percent higher than ECM saturations.

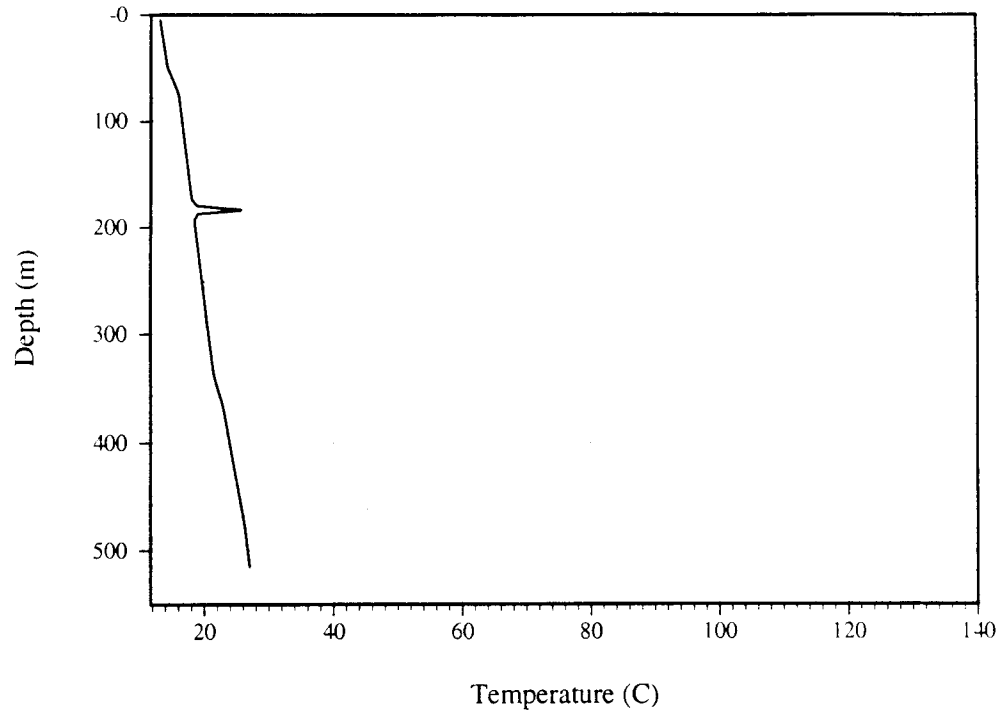


Figure 4-1. Temperature profile for a dual continuum simulation of a drift-scale repository model at 0.1 yr

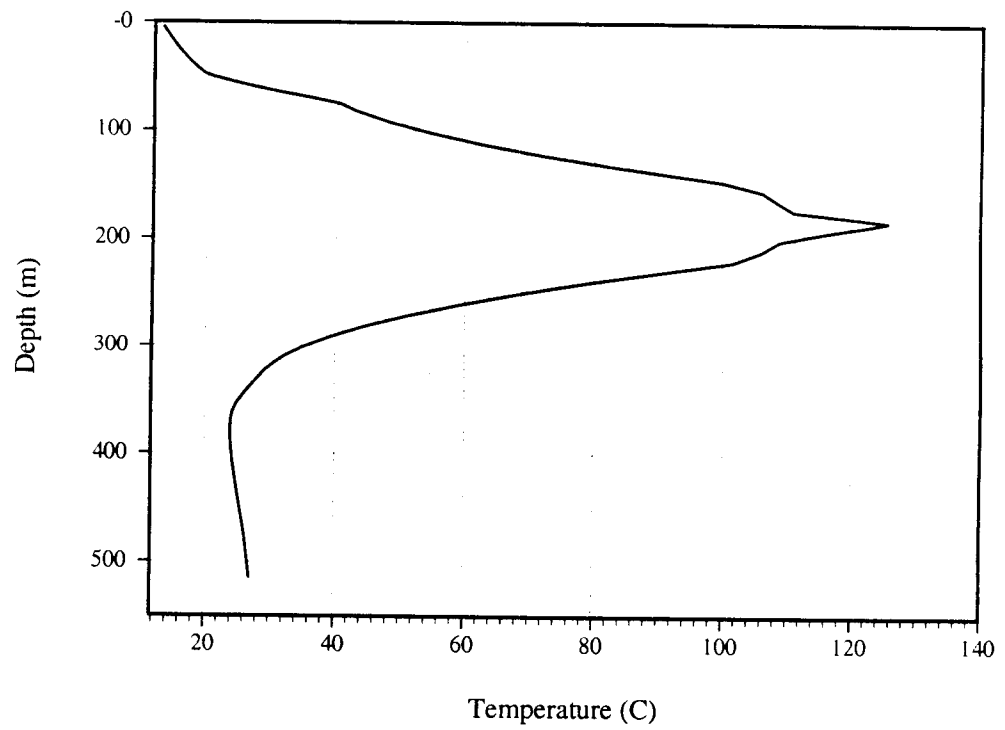


Figure 4-2. Temperature profile for a dual continuum simulation of a drift-scale repository model at 100 yr

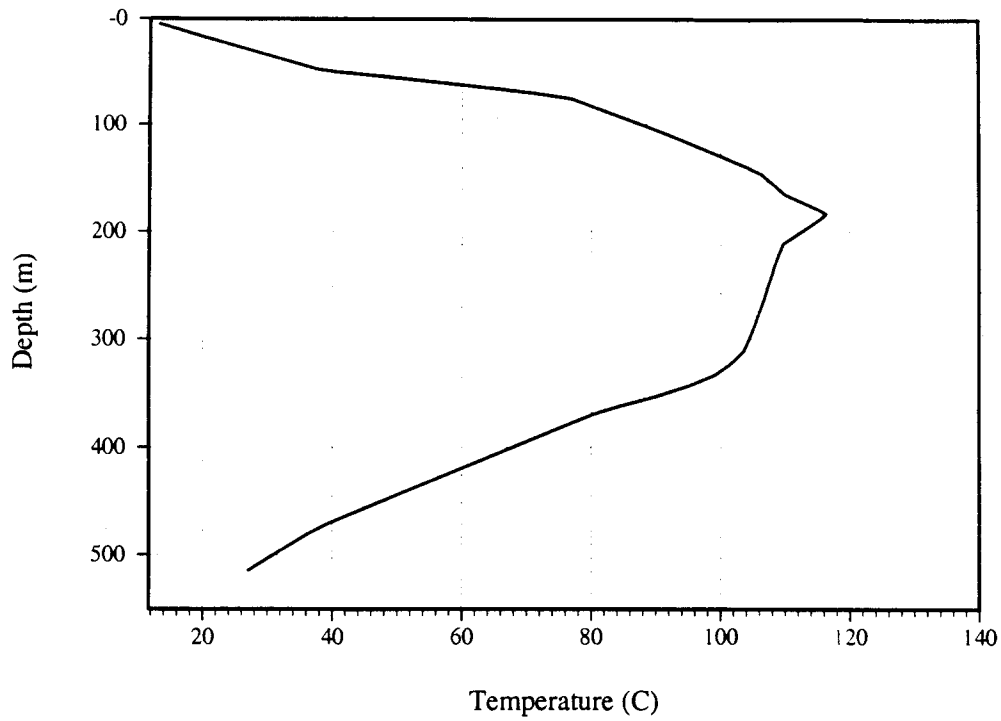


Figure 4-3. Temperature profile for a dual continuum simulation of a drift-scale repository model at 1,000 yr

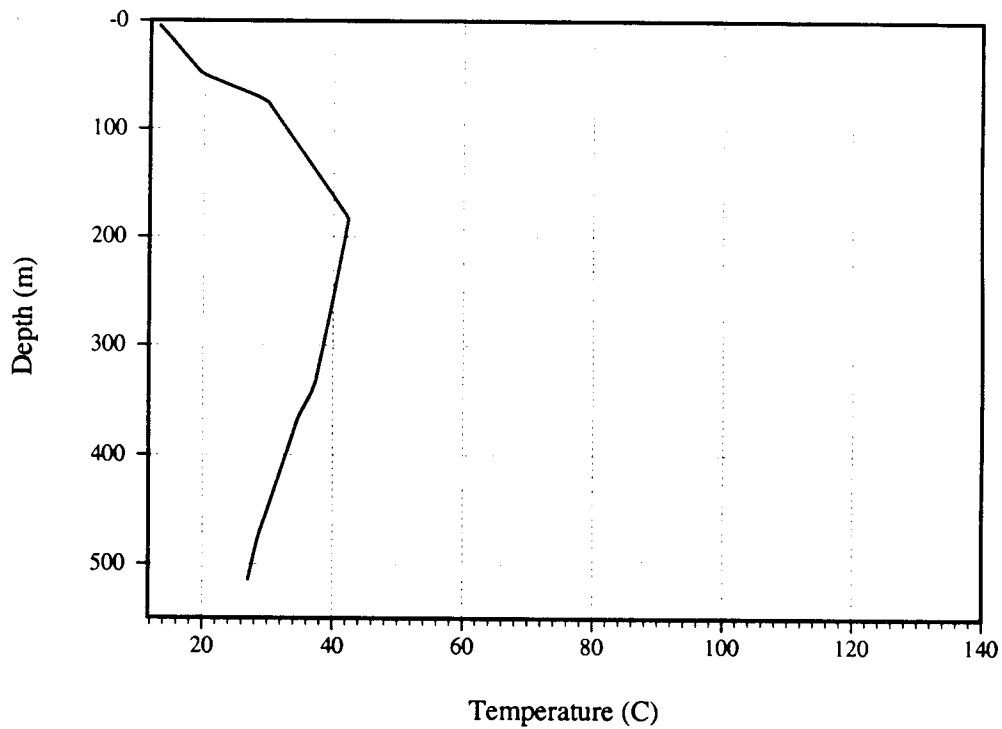


Figure 4-4. Temperature profile for a dual continuum simulation of a drift-scale repository model at 10,000 yr

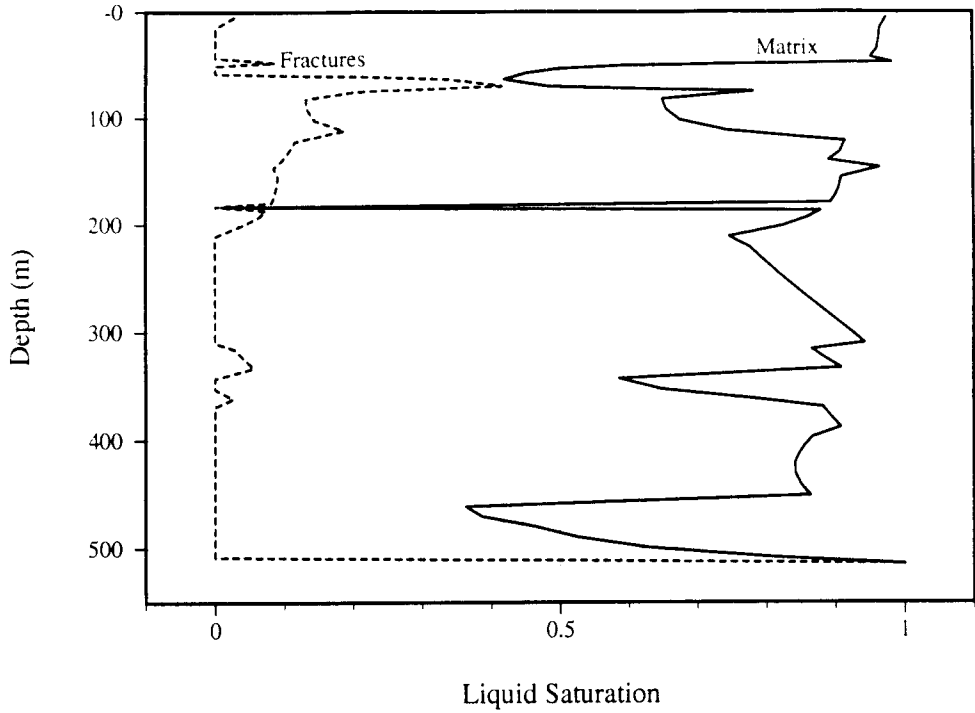


Figure 4-5. Liquid saturation profile for a dual continuum simulation of a drift-scale repository model at 0.1 yr

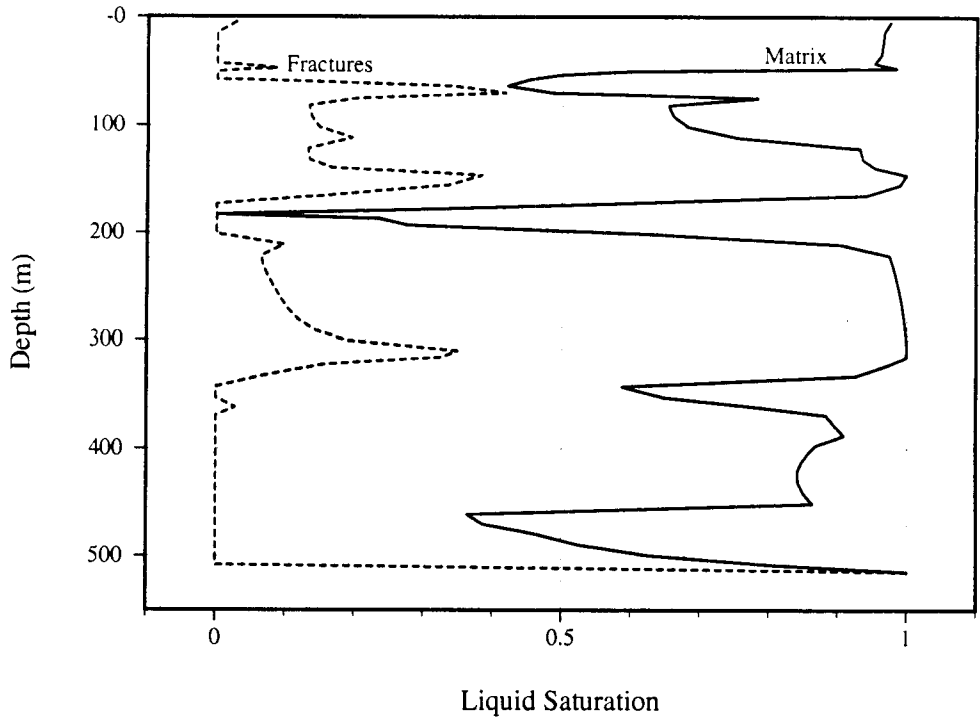


Figure 4-6. Liquid saturation profile for a dual continuum simulation of a drift-scale repository model at 100 yr

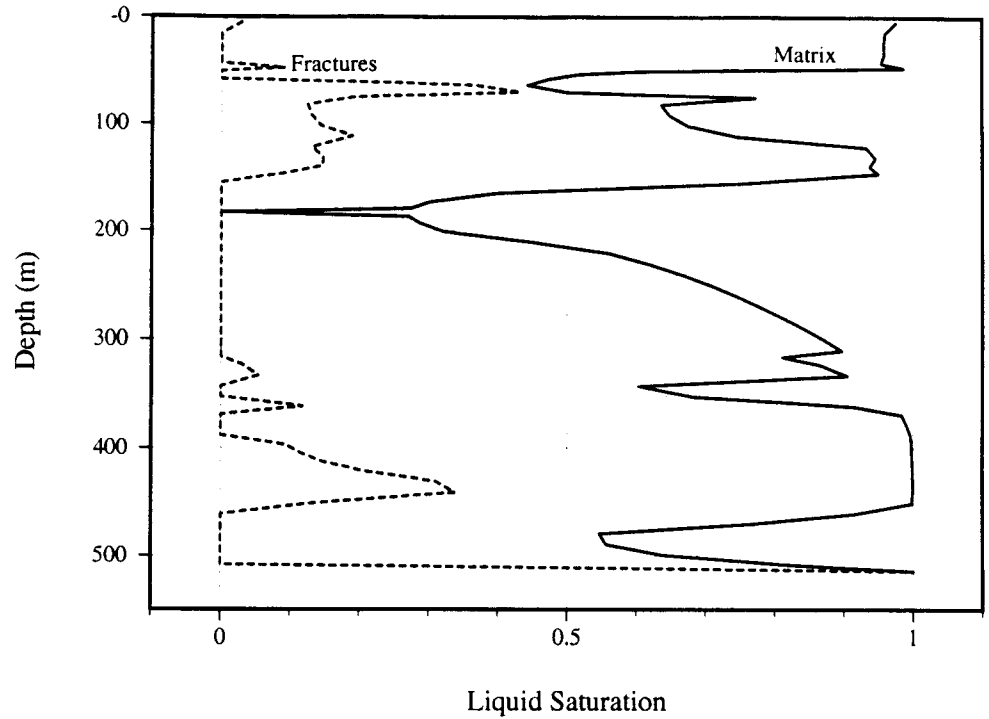


Figure 4-7. Liquid saturation profile for a dual continuum simulation of a drift-scale repository model at 1,000 yr

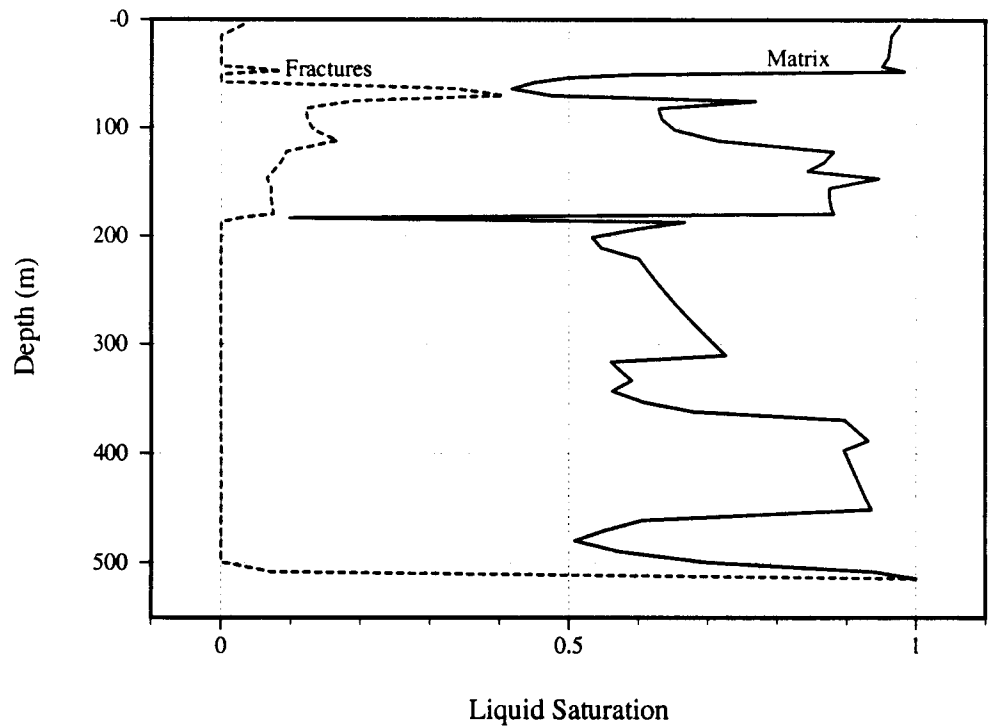


Figure 4-8. Liquid saturation profile for a dual continuum simulation of a drift-scale repository model at 10,000 yr

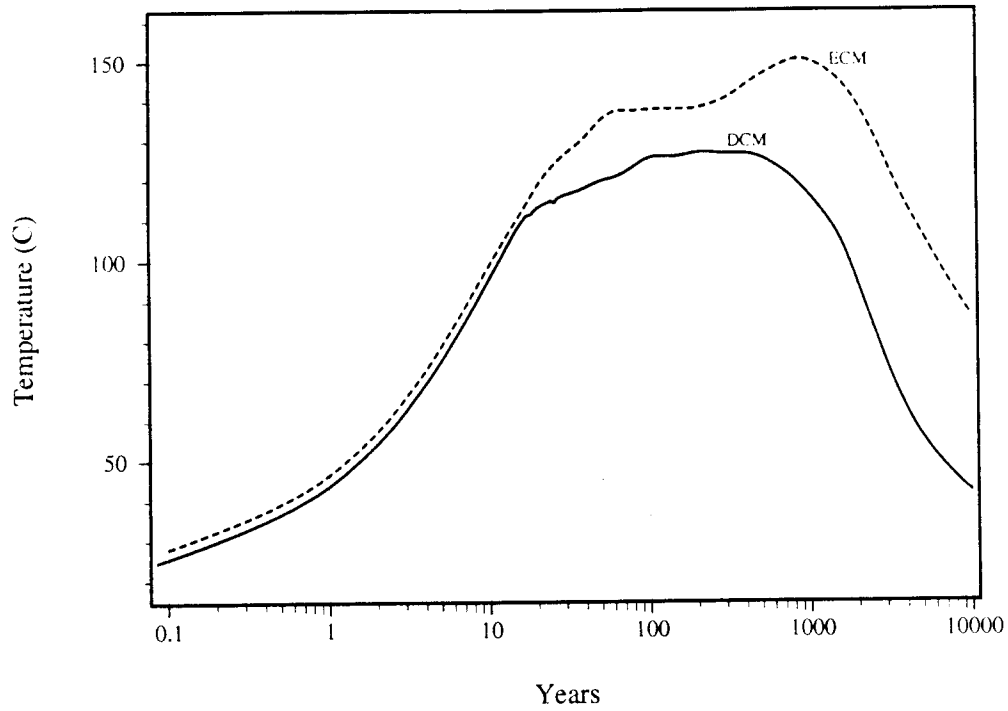


Figure 4-9. Comparison temperature at the waste package predicted for a dual continuum model and an equivalent continuum model

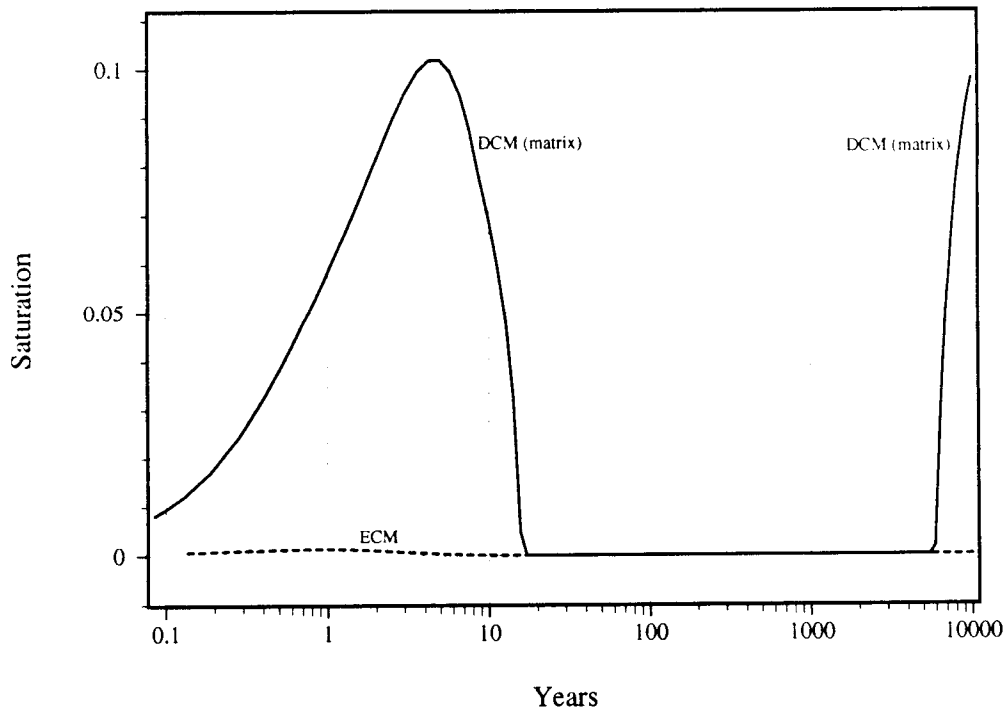


Figure 4-10. Comparison liquid saturation at the waste package predicted for a dual continuum model and an equivalent continuum model

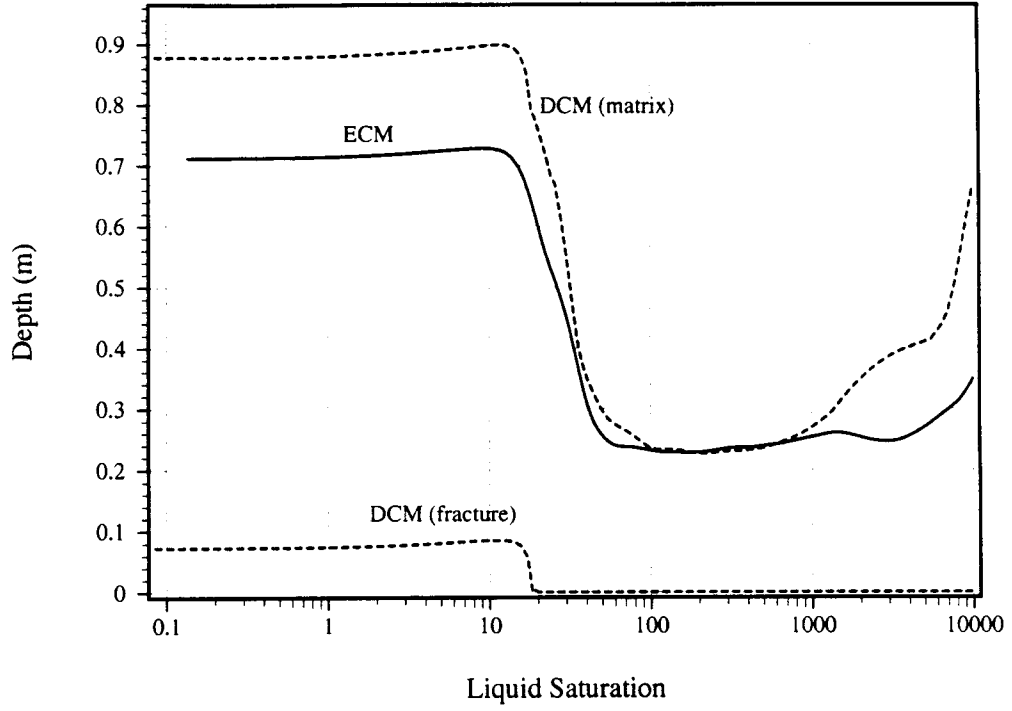


Figure 4-11. Comparison of dual continuum model and equivalent continuum model predictions, liquid saturation 4 m below the waste package

5 REFERENCES

- Andrews, R.W., T.F. Dale, and J.A. McNeish. 1994. *Total System Performance Assessment-1993: An Evaluation of the Potential Yucca Mountain Repository*. B00000000-01717-2200-00099, Rev.01. Las Vegas, NV: Civilian Radioactive Waste Management System, Management and Operating Contractor.
- Birkholzer, J.T., and Y.W. Tsang. 1997. *Pretest Analysis of the Thermal-Hydrological Conditions of the ESF Drift Scale Test*. Berkeley, CA: Lawrence Berkeley National Laboratory.
- Blair, S.C., P.A. Berge, and H.F. Wang. 1996. *Geomechanical Analysis of the Large Block Test*. UCRL-ID-122898. Livermore, CA: Lawrence Livermore National Laboratory.
- Bodvarsson, G.S., and T.M. Bandurraga. 1996. *Development and Calibration of the Three-Dimensional Site-Scale Unsaturated Zone Model of Yucca Mountain, Nevada*. Berkeley, CA: Lawrence Berkeley National Laboratory.
- Bodvarsson, G.S., T.M. Bandurraga, and Y.S. Wu. 1997. *The Site-Scale Unsaturated Zone Model of Yucca Mountain, Nevada, for the Viability Assessment*. Berkeley, CA: Lawrence Berkeley National Laboratory.
- Buscheck, T.A., R.J. Shaffer, and J.J. Nitao. 1997. *Pretest Thermal-Hydrological Analysis of the Drift Scale Test at Yucca Mountain*. Livermore, CA: Lawrence Livermore National Laboratory.
- Francis, N.D., S.R. Sobolik, C.K. Ho, R.R. Eaton, and D. Preece. 1997. *Pre-Experimental Thermal-Hydrological-Mechanical Analyses for the ESF Heated Drift Test*. SLTR97-0002. Albuquerque, NM: Sandia National Laboratories, Nuclear Waste Management Center.
- Glassley, W.E. 1997. *Thermo-Chemical Analyses of the Drift Scale Heater Test: Mineralogical and Geochemical Characteristics*. Level 4 Milestone SP9320M4. Livermore, CA: Lawrence Livermore National Laboratory.
- Ho, C.K., and R.R. Eaton. 1994. *Studies of Thermohydrologic Flow Processes using TOUGH2*. SAND94-2011. Albuquerque, NM: Sandia National Laboratories.
- Klavetter, E.A., and R.R. Peters. 1986. *Estimation of Hydrologic Properties of an Unsaturated, Fractured Rock Mass*. SAND84-2642. Albuquerque, NM: Sandia National Laboratories.
- Lee, K. 1995a. *Progress Report on Pre-Test Calculations for the Large Block Test*, Livermore, CA: Lawrence Livermore National Laboratory.
- Lee, K. 1995b. *Second Progress Report on Pre-Test Calculations for the Large Block Test*, Livermore, CA: Lawrence Livermore National Laboratory.
- Lin, W. 1993. *Technical Basis and Programmatic Requirements for Large Block Testing of Coupled Thermal-Mechanical-Hydrological-Chemical Processes*. Livermore, CA: Lawrence Livermore National Laboratory.

- Lin, W., D. Wilder, S. Blair, T. Buscheck, W. Daily, G. Gdowski, W. Glassley, K. Lee, A. Meike, A. Ramirez, J. Roberts, D. Ruddle, J. Wagoner, D. Watwood, T. Williams, R. Carlson, and D. Neubauer. 1998. An overview of progress on the large block test. *1998 International High-Level Radioactive Waste Management Conference, Las Vegas, NV*, May 11–14, 1998. La Grange Park, IL: American Nuclear Society.
- Seth, M.S., and P.C. Lichtner. 1996. *User's Manual for MULTIFLO: Part I Metra 1.0 β Two-Phase Nonisothermal Flow Simulator*. CNWRA 96–005. San Antonio, TX: Center for Nuclear Waste Regulatory Analyses.
- TRW Environmental Safety Systems, Inc. 1995. *Total System Performance Assessment–1995: An Evaluation of the Potential Yucca Mountain Repository*. B00000000–0171702200-00136, Rev. 01. Las Vegas, NV: TRW Environmental Safety Systems, Inc.
- TRW Environmental Safety Systems, Inc. 1997. *Drift Scale Test Design and Forecast Results*. Civilian Radioactive Waste Management System, Management & Operating Contractor. Las Vegas, NV: U.S. Department of Energy, Yucca Mountain Site Characterization Office.
- Wang, J.S.Y., and C.F. Ahlers. 1996. *Pre-Test Analysis of the Large Block Test—Air Flow and Gas Tracer Transport for Thermal-Hydrological Evaluation*. Berkeley, CA: Lawrence Berkeley National Laboratory.
- Wilder, D.B. 1997. *Near-Field and Altered-Zone Environment Report: Volume I, Technical Basis for EBS Design*. UCRL–LR–107476, Rev. 1. Livermore, CA: Lawrence Livermore National Laboratory.
- Wilder, D.B., W. Lin, S.C. Blair, T. Buscheck, R.C. Carlson, K. Lee, A. Meike, A.L. Ramirez, J.L. Wagoner, and J. Wang. 1997. *Large Block Test Status Report*. Livermore, CA: Lawrence Livermore National Laboratory.
- Wilson, M.L., J.H. Gauthier, R.W. Barnard, G.E. Barr, H.A. Dockery, E. Dunn, R.R. Eaton, D.C. Guerin, N. Lu, M.J. Martinez, R. Nelson, C.A. Rautman, T.H. Robey, B. Ross, E.E. Lewis, A.D. Lamont, I.R. Triay, A. Meijer, and D.E. Morris. 1994. *Total System Performance Assessment for Yucca Mountain - SNL Second Iteration (TSPA-93)*. SAND93-2675. Albuquerque, NM: Sandia National Laboratory.

**ADDITIONAL INFORMATION FOR THERMAL-HYDROLOGIC MODELING
PROGRESS REPORT**

Document Date:	05/29/1998
Availability:	Southwest Research Institute® Center for Nuclear Waste Regulatory Analyses 6220 Culebra Road San Antonio, Texas 78228
Contact:	Southwest Research Institute® Center for Nuclear Waste Regulatory Analyses 6220 Culebra Road San Antonio, TX 78228-5166 Attn.: Director of Administration 210.522.5054
Data Sensitivity:	<input checked="" type="checkbox"/> "Non-Sensitive" <input type="checkbox"/> Sensitive <input type="checkbox"/> "Non-Sensitive - Copyright" <input type="checkbox"/> Sensitive - Copyright
Date Generated:	06/02/1998
Operating System: (including version number)	Solaris
Application Used: (including version number)	TAR Archive
Media Type: (CDs, 3 1/2, 5 1/4 disks, etc.)	1 - 3 1/2 disk
File Types: (.exe, .bat, .zip, etc.)	Various
Remarks: (computer runs, etc.)	Media contains: Data run outputs